3. SITE 430: ŌJIN SEAMOUNT

Shipboard Scientific Party[1]

SITE DATA, HOLE 430

Date Occupied: 1 August 1977 (0900 Z)

Date Departed: 1 August 1977 (2013 Z)

Time on Hole: 11 hours, 13 minutes

Position: 37°58.88′N, 170°35.45′E

Water Depth (sea level): 1444.8 corrected meters, echo sounding

Water Depth (rig floor): 1454.8 corrected meters, echo sounding

Bottom Felt at: 1464.0 meters, drill pipe

Penetration: 14.0 meters

Number of Holes: 1

Number of Cores: 3

Total Length of Cored Section: 14.0 meters

Total Core Recovery: 7.9 meters

Percentage Core Recovery: 56.4

Oldest Sediment Cored:
Depth sub-bottom: 14.0 meters
Nature: Pebbly mudstone
Chronostratigraphy: Mixed Holocene to upper Eocene
Measured velocity: 1.8 to 2.0 km/s

Basement: Not reached

Principal Results: Three holes were drilled into what appeared, on the site survey seismic records, to be a lagoonal sediment pond on Ōjin Seamount. Hole 430 was abandoned because of caving, after recovery of three cores (14 m) of pebbly mudstone which contain a variety of angular to rounded clasts ranging from siltstone to basalt and Recent to Eocene shallow-water fossil assemblages. (See Table 1 for coring summary of the holes drilled at Site 430.) Geophysical records suggest that we may have drilled into a small landslide.

[1] Everett D. Jackson (Co-Chief Scientist), United States Geological Survey, Menlo Park, California; Itaru Koizumi (Co-Chief Scientist), Osaka University, Osaka, Japan; R. James Kirkpatrick, Deep Sea Drilling Project, Scripps Institution of Oceanography, La Jolla, California (now at University of Illinois, Urbana, Illinois); Gennady Avdeiko, USSR Academy of Sciences, Petropavlovsk-Kamchatsky, USSR; David Clague, Middlebury College, Middlebury, Vermont; G. Brent Dalrymple, United States Geological Survey, Menlo Park, California; Anne-Marie Karpoff, Institut de Geologie, Strasbourg, France; Judith McKenzie, Eidg. Technische Hochschule, Zürich, Switzerland; Arif Butt, Universitat Tübingen, Tübingen, Federal Republic of Germany; Hsin Yi Ling, University of Washington, Seattle, Washington; Toshiaki Takayama, Kanazawa University, Kanazawa, Japan; H. Gary Green, United States Geological Suivey, Menlo Park, California; Jason Morgan, Princeton University, New Jersey; and Masaru Kono, University of Tokyo, Tokyo, Japan.

TABLE 1
Coring Summary, Site 430

Core	Date (Aug. 1977)	Time	Depth from Drill Floor (m)	Depth below Sea Floor (m)	Length Cored (m)	Length Recovered (m)	Recovery (%)
Hole 430							
1	2	0245	1464.0-1466.5	0.0-2.5	2.5	0.0	0.0
2	2	0405	1466.5-1468.5	2.5-4.5	2.0	0.7	38.5
3	2	0630	1468.5-1478.0	4.5-14.0	9.5	0.2	2.0
Total					14.0	0.9	56.4
Hole 430A							
1	2	0821	1485.5-1491.0	0.0-5.5	5.5	1.03	19.0
Washed			1491.0-1504.5	5.5-19.0			
2	2	0935	1504.5-1514.0	19.0-28.5	9.5	.64	7.0
Washed			1514.0-1523.5	28.5-38.0			
3	2	1027	1523.5-1533.0	38.0-47.5	9.5	.30	3.0
Washed			1533.0-1542.5	47.5-57.0			
4	2	1230	1542.5-1552.0	57.0-66.5	9.5	2.03	21.0
		1320		Cavings		2.0	
5	2	1550	1552.0-1561.5	66.5-76.0	9.5	7.90	83.0
6	2	2120	1561.5-1571.0	76.0-85.5	9.5	4.58	48.0
7	3	0133	1571.0-1580.5	85.5-95.0	9.5	0.0	0.0
8	3	0323	1580.5-1590.0	95.0-104.5	9.5	0.0	0.0
9	3	0504	1590.0-1599.5	104.5-114.0	9.5	0.0	0.0
10	3	0812	1599.5-1602.5	114.0-117.0	3.0	0.30	10.0
11	3	1100	1602.5-1603.5	117.0-118.0	1.0	0.05	5.0
Total					85.5	16.83	19.7
Hole 430B							
1	3	1315	1492.0-1495.0	0.0-3.0	3.0	0.1	3.0

SITE DATA, HOLE 430A

Date Occupied: 1 August 1977 (2005 Z)(2 August 1977 [0705 L])

Date Departed: 2 August 1977 (2348 Z) (3 August 1977 [1048 L])

Time on Hole: 27 hours, 43 minutes

Position: 37°59.29′, 170°35.86′E

Water Depth (sea level): 1478.8 corrected meters, echo sounding

Water Depth (rig floor): 1488.8 corrected meters, echo sounding

Bottom Felt at: 1485.5 meters, drill pipe

Penetration: 118.0 meters

Number of Holes: 1

Number of Cores: 11

Total Length of Cored Section: 85.5 meters

Total Core Recovery: 16.83 meters

Percentage Core Recovery: 19.7

Oldest Sediment Cored:
Depth sub-bottom: 59.3 meters
Nature: Volcaniclastic
Chronostratigraphy: Upper Paleocene
Measured velocity: 2.8 km/s

Basement:
Depth sub-bottom: 59.3 meters
Nature: Highly vesicular to very massive basalt
Velocity range: 4.5–5.8 km/s

Principal Results: Hole 430A was offset on beacon 3000 feet at 040° true from Hole 430. The hole was spudded into siltstone containing a few basaltic pebbles, and this material proved much easier to core than the surface debris at Hole 430. The drill penetrated 47.5 meters of calcareous ooze and sand, interbedded near the base with 11.8 meters of volcaniclastic sand and ash. These sediments contain upper Paleocene to lower Eocene foraminifers and upper Paleocene nannofossils, as well as benthic foraminifers, ostracodes, and calcareous algae typical of shallow-water reef environments. Both sediments and fossils demonstrate that Ōjin Seamount is capped by Paleocene–Eocene lagoonal deposits, as predicted, and that Ōjin Seamount is older than Kōkō Seamount to the south. Immediately beneath the black volcaniclastic sands, five flow units of subaerially erupted basalts were cored to a total depth of 85.5 meters. The upper four flow units are very vesicular to massive hawaiite, whereas the lower flow unit is fresh tholeiitic basalt. These flows indicate that Ōjin Seamount is a Hawaiian-type edifice with alkalic stage lavas overlying shield-building tholeiitic basalt. Natural remanent magnetization in both volcaniclastic sand and basalts is stable, and indicates the magnetic field inclinations when these rocks formed. The inclinations in the upper four flow units are very similar, suggesting that the eruptions of these flows took place in a very short time.

SITE DATA, HOLE 430B

Date Occupied: 3 August 1977 (0036 Z) (3 August 1977) [1136 L])

Date Departed: 3 August 1977 (0712 Z) (3 August 1977) [1812 L])

Time on Hole: 6 hours, 36 minutes

Position: 37°59.52′N, 170°36.12′E

Water Depth (sea level): 1470.8 corrected meters, echo sounding

Water Depth (rig floor): 1480.8 corrected meters, echo sounding

Bottom Felt at: 1492.0 meters, drill pipe

Penetration: 3.0 meters

Number of Holes: 1

Number of Cores: 1

Total Length of Cored Section: 3.0 meters

Total Core Recovery: 0.10 meters

Percentage Core Recovery: 3.0

Oldest Sediment Cored:
Depth sub-bottom: 3.0 meters
Nature: Watery foraminifer sand
Chronostratigraphy: Quaternary
Measured velocity: 1.5 km/s

Basement: Not reached

Principal Results: Since a satisfactory surface sample was not collected at either Hole 430 or Hole 430A, owing to mixing during coring operations, we offset 1640 feet at 040° true, to avoid cuttings, and dropped the drill string to attempt a punch core at this site. We were at that time unaware that the drill bit was completely blocked by basalt cobbles, and we obtained only about 10 cm of watery ooze. The fossils in the ooze proved to be Quaternary; fossils representing the Neogene/Paleogene boundary appear to have been completely washed away at this site.

OPERATIONS

Pre-Drilling Site Survey

A 80-kJ sparker profile taken by the R/V *S. P. Lee* along the long axis (oriented northeast-southwest) of Ōjin Seamount (Figure 1) on 9 October 1976 indicated that the flat-topped seamount is probably capped by marine terrace deposits, drowned coral reefs, and perhaps locally by lagoonal sediments (Figure 2). The subsurface stratigraphy at the first of the two proposed drilling sites (Site 55-6) appears in this profile as a gently dipping stratified unit fringing the southwest edge of the top of the seamount. A well-defined acoustic basement underlies (probable) stratified terrace deposits which vary in thickness from a few meters to well over 100 meters. The second site (55-6A) is in what appears to be a large central topographic depression containing as much as several hundred meters of lagoonal and reef bank strata. A distinct, U-shaped, acoustic basement basin filled with flat-lying strata lies in the deepest part of this depression. Site 55-6A was originally considered more promising, but we could not resolve acoustic basement here from the *Lee* site survey profile. Neither site showed much penetration on the 3.5-kHz profile shot in the area surveyed by the R/V *S. P. Lee* (Figure 3).

We therefore decided to traverse the sediment pond at Site 55-6A and to drill there if basement could be resolved. If it could not, we planned to occupy and drill Site 55-6, where we knew the depth to acoustic basement.

We steamed for 1906 nautical miles on a rhumbline course of 301° true from Honolulu, Hawaii to a point near the eastern edge of Ōjin Seamount, at 37°57′N latitude and 170°50′N longitude (Figure 1). At this point we changed course to 290° true to obtain a seismic reflection profile along a course approximately perpendicular to the *Lee* crossing. We reduced speed — to reduce noise and exaggeration of the seismic profiles — from about 10 knots to 7.7 knots at 1831 Z, 31 July (0531 L, 1 August) 1977, at latitude 37°54′N and longitude 171°19.25′E, 3 hours, 21 minutes before turning onto course 290° true. The first crossing of proposed Site 55-6A airgun profiles showed that the acoustic basement lay beneath 0.15 and 0.25 s of well-layered strata within the basin (Figures 4 and 5). The 3.5-kHz profile (Figure 6) on this crossing did not show any acoustic transparency that would indicate a cover of soft pelagic muds. Nevertheless, we had no other reason to suppose that the hole could not be drilled. To define the shape of the sediment pond, we proceeded past Site 55-6A on a course of 290° true, passing approximately 0.5 nautical miles northeast of Site 430, at 2314 Z, 31 July (1014 L, 1 August) 1977. We continued on course for about 20 miles, to latitude 28°08′N, longitude 170°11′E, and at 0200 Z (1300 L), 1 August 1977,

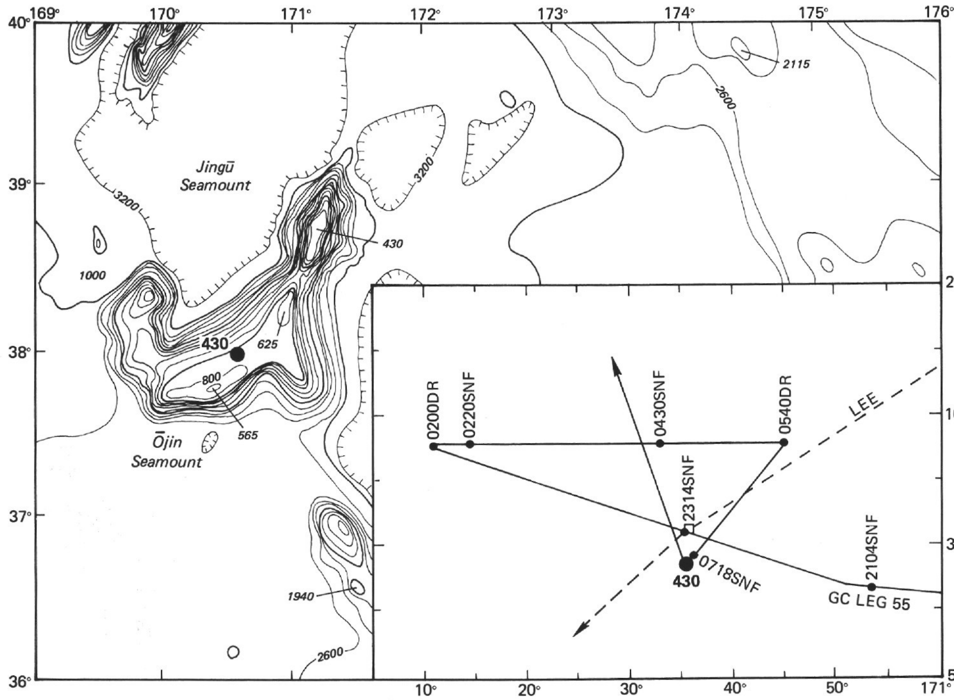

Figure 1. *Bathymetry of Ōjin and Jingū seamounts, showing the* Glomar Challenger *Leg 55 and* S. P. Lee *8-76 NP tracks. Depths in fathoms. Bathymetry after Chase et al. (1970).*

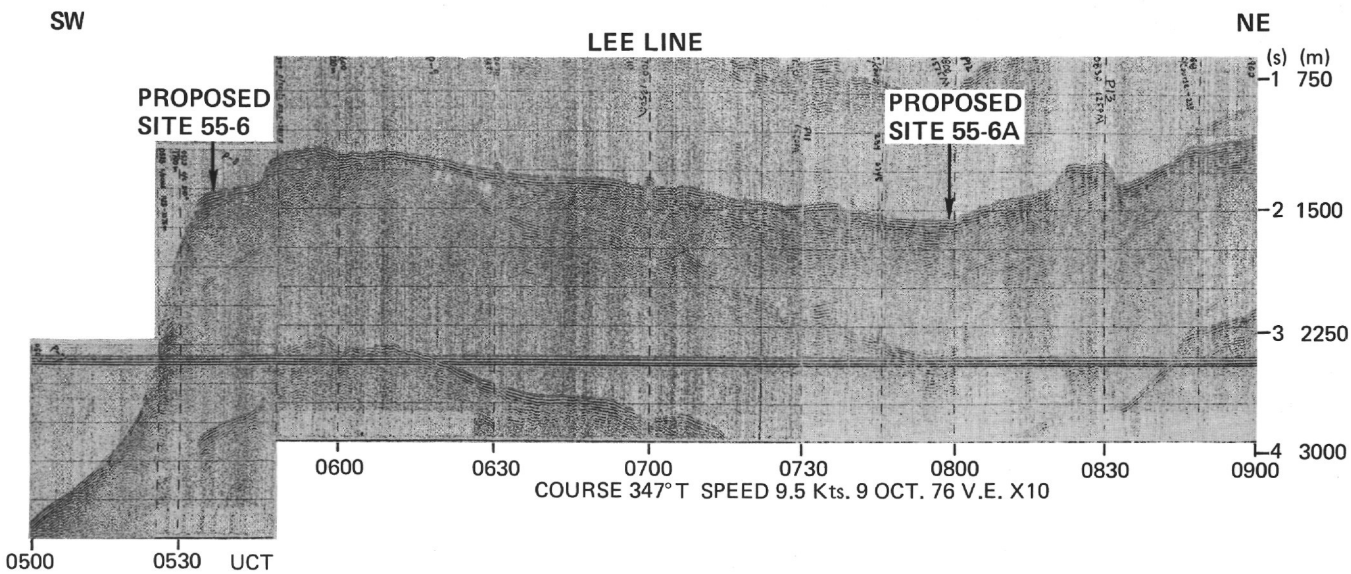

Figure 2. *U.S. Geological Survey's* S.P. Lee *seismic reflection profile, showing locations of the originally proposed Sites 55-6 and 55-6A.*

turned eastward to a course of 090°true. We ran at a speed made good (SMG) of 7.2 knots until 0540 Z (1640 L), 1 August 1977, 38°08′N latitude and 170°45′E longitude, to intercept and reoccupy the *Lee* survey line. We then turned to a course of 220° true and maintained 6.8 knots SMG for about 1 hour 15 minutes, at which time we slowed to 4.0 knots SMG and continued on course until we passed over Site 430. The maneuvers defined the small irregular sedimentary basin where Site 55-6A had originally been located (Figures 7 through 10). The 3.5-kHz record near Site 430 showed 0.015 s of hashy transparency which suggested that a layer of unconsolidated material covered firmer strata (Figure 10). We dropped the beacon at Site 430, continued on course past the site for 10 minutes, and then looped back to position the ship over the beacon. On our final ap-

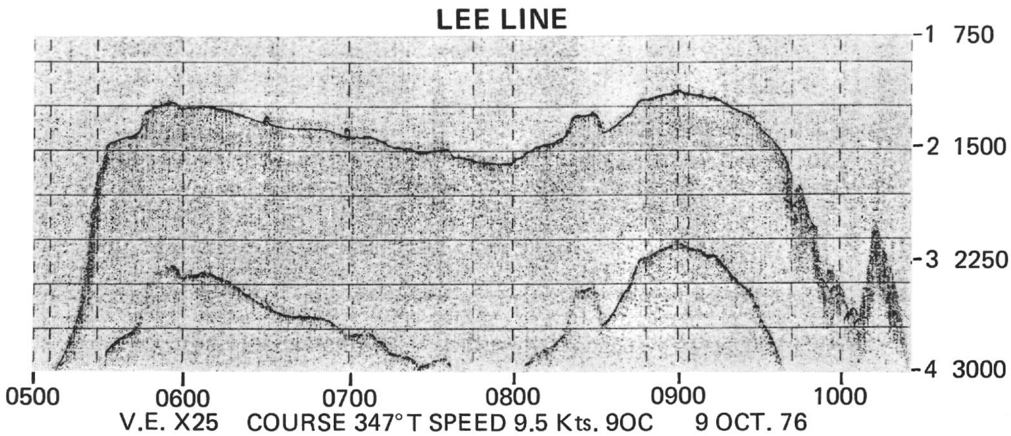

Figure 3. *U. S. Geological Survey's* S. P. Lee *3.5-kHz profile, showing locations of the originally proposed Sites 55-6 and 55-6A.*

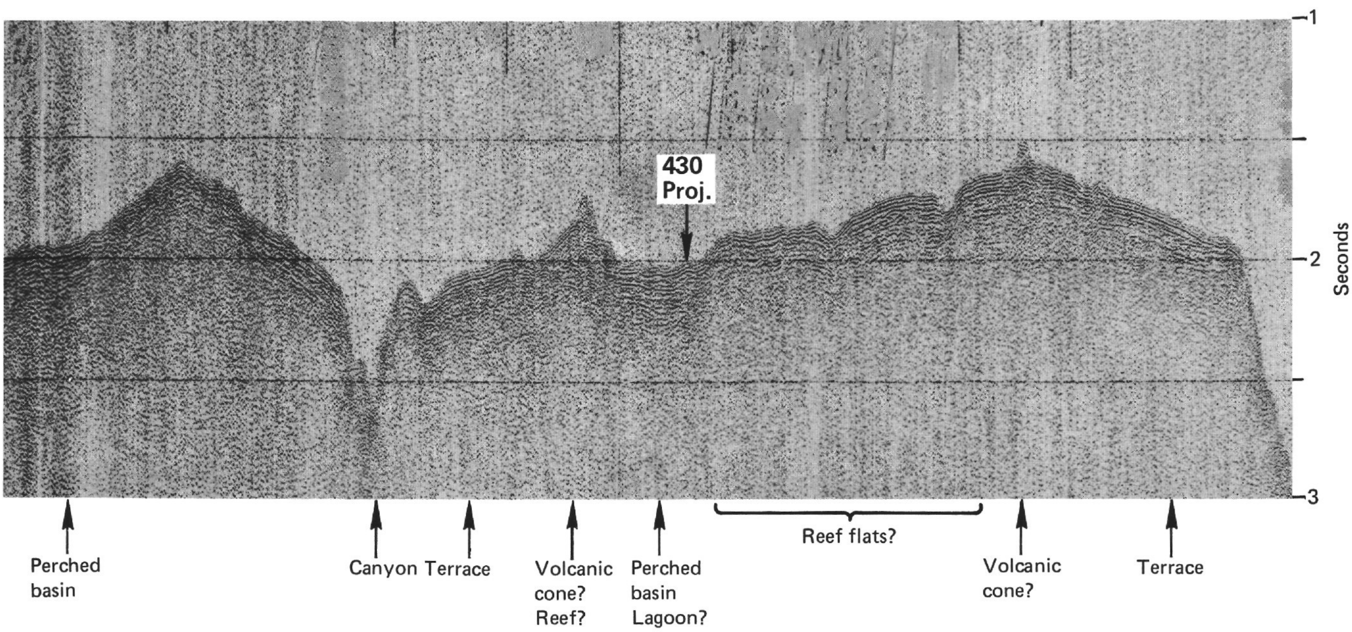

Figure 4. Glomar Challenger *5-s seismic reflection profile across proposed Site 55-6A, showing physiographic features used in locating Site 430.*

proach to the beacon, the sea floor shoaled from about 2.0 s to 1.95 s; an assumed average velocity of 1500 m/s gives a thickness for the shoal of about 38 meters, which is enough soft sediment to safely bury the bottom-hole assembly.

Site 430 proved to be on a flat basin floor near the base of a slope rising gently toward the northeast. Subsurface reflectors within the basin were generally flat-lying, except near the edge of the basin where they gently lapped onto acoustic basement. A bubble pulse of about 0.05 s masked the upper part of the section, but the reflectors below the bubble pulse were well defined, continuous, and lapped onto the irregular acoustic basement surface, forming buttress unconformities. The slope surrounding the sedimentary basin showed displaced, rotated, and contorted reflectors, suggesting downslope sediment creep or slumping of surficial deposits.

Drilling Operations

At 0730 Z (1830 L), 1 August 1977, we dropped a 16-kHz beacon at 37°58.88'N, 170°45'E,[2] near the edge of the sediment pond in which preliminary Site 55-6A had been located. At the beacon drop site, a small mound appeared on the 3.5-kHz records (Figure 9), indicating the presence of unconsolidated sediments. We decided to drill directly on that site, again positioned the ship over the beacon at 0848 Z (1948 L), dropped the drill string, and felt bottom in 1464 meters of water at

[2] See Table 2 for on-site satellite navigation positions.

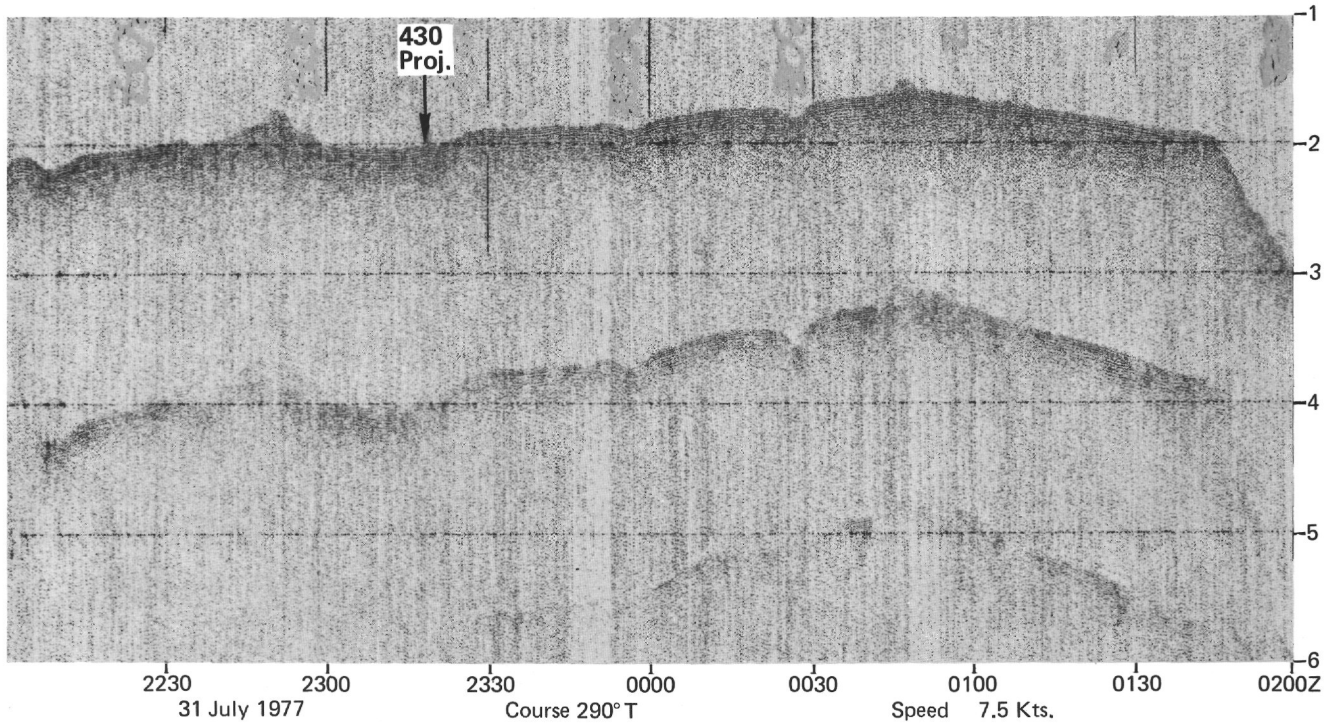

Figure 5. Glomar Challenger *10-s seismic reflection profile across proposed Site 55-6A, showing projected location of Site 430.*

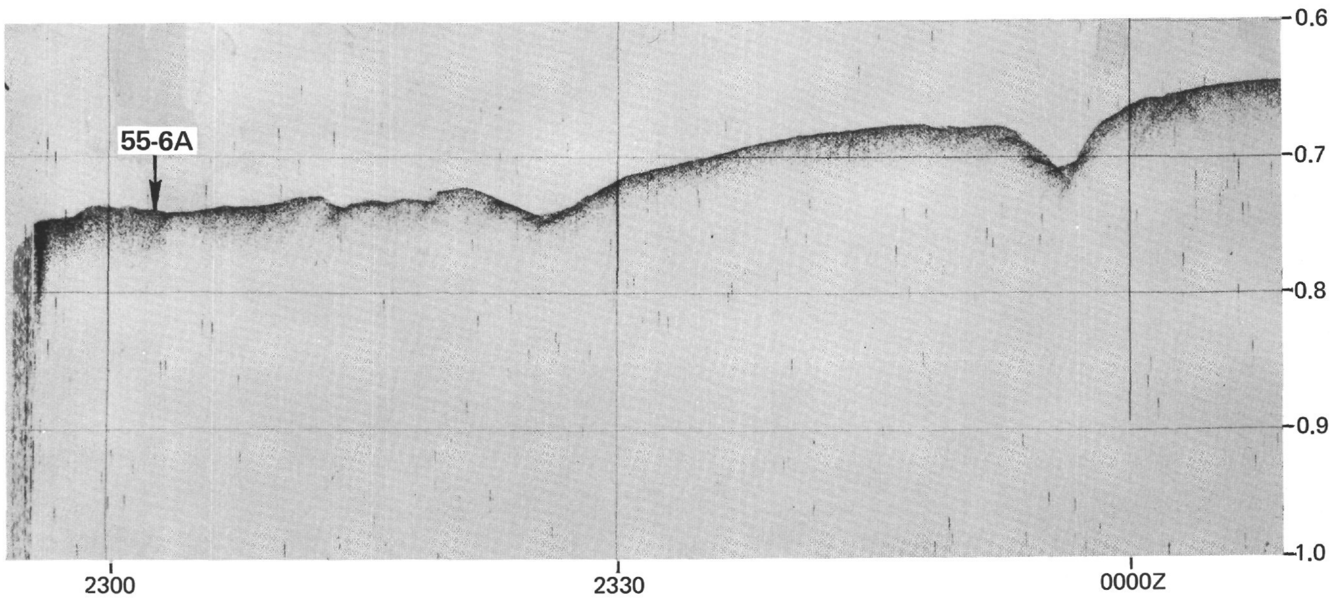

Figure 6. Glomar Challenger *3.5-kHz profile across proposed Site 55-6A, showing lack of acoustic transparency.*

1300 Z (0000 L, 2 August). Bottom was firm, but offered little resistance to the drill, and 2.5 meters was cored without assistance of the power sub. Material recovered at Hole 430 was pebbly mudstone with a very pasty consistency and many angular to rounded clasts that promised to be difficult to drill. At a penetration depth of 14.0 meters, the hole caved in, and it was apparent that the unit could not be held for drilling.

At 1930 Z (0630 L, 2 August), we requested an offset on beacon of 3000 feet at 040° true. The bottom-hole assembly was raised above mudline, and the offset was completed at 2005 Z (0705 L, 2 August). We spudded in on Hole 430A at 2050 Z (0750 L, 2 August). Drilling was considerably easier here, and although a small interval of pebbly mudstone was cored, the drill soon penetrated calcareous muds, soft algal limestones, and volcani-

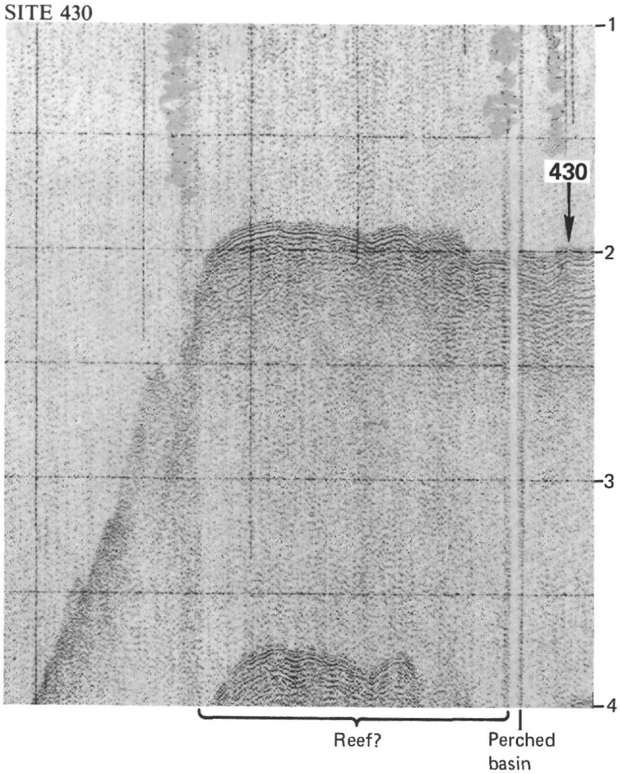

Figure 7. Glomar Challenger *5-s seismic reflection profile on approach to Site 430 (see Figure 1).*

clastic sandstones. As drilling proceeded, alternate sections were washed to bury the bottom-hole assembly expeditiously. Penetration was 66.5 meters in this interval. Core recovery in the interval was poor (12%); the sediments cored were much less indurated than we had anticipated, and this contributed to our overestimate of sedimentary thickness from our acoustic records. Upon steaming off site, we found that our offset had put us in a shallower part of the sediment pond than at the beacon drop site.

At 59.3 meters below mudline we entered basaltic basement, and penetrated nothing but basalt to our final penetration depth of 118 meters. Core 430A-5 contained 7.90 meters of hard basalt. Core 430A-6 contained only 3.55 meters, and we observed that the plastic core liner at the base of Section 1 was deformed and torn. As the driller began to cut Core 430A-7, the bit appeared to be plugged, and efforts were made to dislodge what was thought to be a wedged basalt fragment. These efforts appeared successful, and we resumed drilling. We then drilled three 9.5-meter intervals, but recovered no core. At first we thought this resulted from the bit passing through fine breccia or other noncorable formations, especially because the drilling rate increased somewhat. Drilling pressure on the bit had also increased, however, during drilling of intervals 430A-7, 430A-8, and 430A-9, as a consequence of the second bumper sub of the bottom-hole assembly having been closed during drilling of Core 430A-6. The lack of

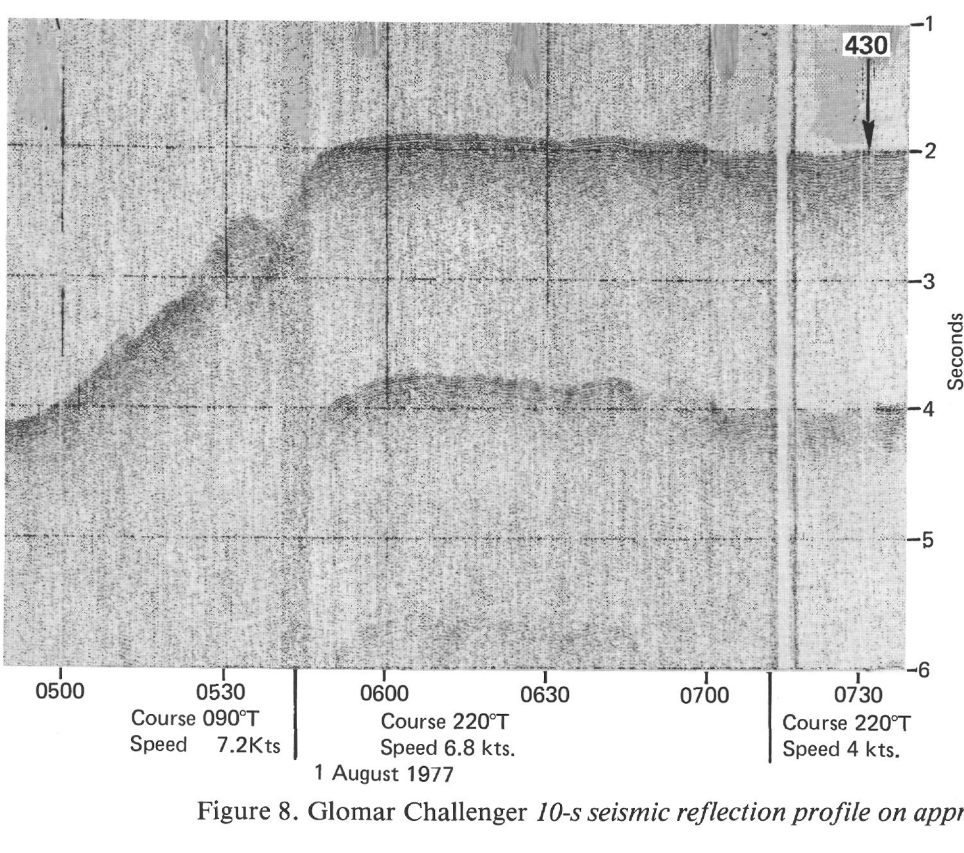

Figure 8. Glomar Challenger *10-s seismic reflection profile on approach to Site 430.*

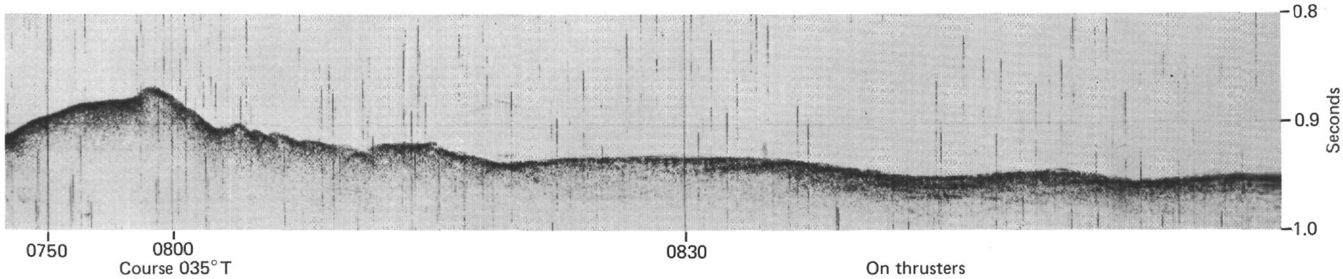

Figure 9. Glomar Challenger *3.5-kHz profile on approach to Site 430.*

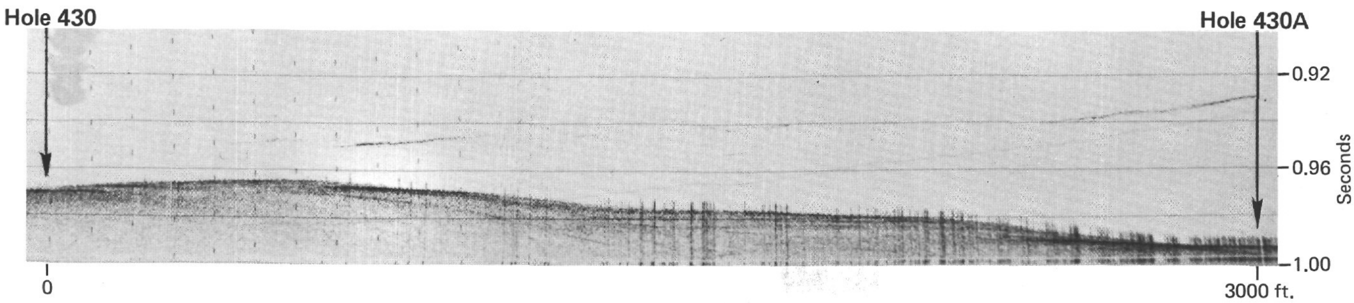

Figure 10. Glomar Challenger *3.5-kHz profile obtained during offset between Holes 430 and 430A, showing bottom configuration and layering within the shallow surficial materials.*

TABLE 2
On-Site Satellite Navigation Positions, Site 430

	Time (Z)	Latitude	Longitude	Satellite	Statistics	Altitude
Hole 430						
430-1	1 Aug. 1050	37°59.568'N	170°36.447'E	19	Poor	16°
430-2	1138	37°59.267'N	170°36.447'E	20	Very poor	31°
430-3	1248	37°58.919'N	170°37.122'E	13	Very poor	19°
430-4	1324	37°59.126'N	170°34.762'E	20	Very poor	36°
Hole 430A						
430A-1	1 Aug. 2202	37°59.134'N	170°36.723'E	19	Very poor	31°
430A-2	2326	37°59.280'N	170°36.741'E	20	Very poor	30°
430A-3	2 Aug. 0000	37°59.274'N	170°36.883'E	13	Fair	42°
430A-4	0520	37°59.279'N	170°35.863'E	12	Excellent	31°
430A-5	0706	37°59.300'N	170°35.857'E	12	Good	38°
430A-6	0814	37°59.298'N	170°35.853'E	19	Excellent	39°
430A-7	1000	37°59.303'N	170°35.857'E	19	Excellent	35°
430A-8	1020	37°59.298'N	170°35.858'E	14	Fair-Good	68°
430A-9	1200	37°59.282'N	170°35.866'E	13	Good	43°
430A-10	1220	37°59.293'N	170°35.847'E	20	Good	70°
430A-11	1404	37°59.325'N	170°35.850'E	20	Excellent	16°
430A-13	1716	37°59.276'N	170°35.861'E	12	Excellent	30°
430A-15	1902	37°59.239'N	170°35.758'E	12	Good	39°
430A-16	1928	37°59.269'N	170°35.883'E	19	Poor-Fair	13°
430A-17	2138	37°59.298'N	170°35.866'E	14	Good	32°
Hole 430B						
430B-1	3 Aug. 0006	37°59.110'N	170°35.518'E	20	Poor	62°

pump pressure indicated that a pump valve in the bottom-hole assembly was lodged open, perhaps because of damage or failure, or because the bit was jammed above the cones and the core barrel would not seat. We drilled a 2-meter section that contained moderately weathered basalt chips in the core catcher of Core 430A-10. We then drilled a 1-meter section that contained chips of very hard basalt in the core catcher of Core 430A-11. During this small drilling interval, a bit bearing appeared to have frozen, and we decided to abandon the hole at 0000 Z (1100 L, 3 August). When the string was pulled, we found about a dozen abraded pieces of basalt, ranging in size from 3 to 10 cm, lodged in the bit above the cones (Figure 11). Apparently the inner core catcher of Core 430A-6 had failed and allowed the lower several meters of basaltic core to fall in and jam the bit. Thereafter, the core barrel failed to seat, because large angular pieces of basalt could neither be shaken from the bit nor retrieved by the core catcher.

While we were drilling interval 430A-9, the 16-kHz beacon showed signs of failure; at 1822 Z on 2 August (0522 L, 3 August), we dropped a 13.5-kHz beacon and assumed positioning control in the semi-automatic mode. The ship remained on beacon over Hole 430A during drilling.

Since one of our objectives was to compare Quaternary fauna and flora from the Emperor Seamount drilling sites, we decided to attempt a final punch core before leaving Site 430. We pulled the drill string above mudline and offset the ship 1640 feet at 040° true to avoid the area of cuttings from Hole 430A. We spudded in the bit at 0145 Z (1245 L), 3 August, and worked 3.0 meters into the surface, using the power sub, but with all pumps closed. We recovered about 0.1 meter of watery ooze, but several cubic centimeters of calcareous ooze adhered to the drill bit; these were identified as part of the punch core, because the bits had not rotated since the material was acquired.

We left Site 430 at 0712 Z (1812 L), 3 August, after spending a total of 46 hours and 12 minutes on site.

Post-Drilling Operations

After leaving Hole 430B, we circled toward the southeast and passed over Hole 430A at 0752 Z (1852 L), 3 August 1977, on course 341° true at 6 knots (Figure 12). The last seismic profile shows the position of Hole 430A to be on the northeast slope above the basin floor, and to have only about 0.1 s of sediments

Figure 11. *Bit from Hole 430A after recovery on deck. The core catcher had failed during recovery of Core 6. A single 20-cm piece of core was removed before this photograph was taken.*

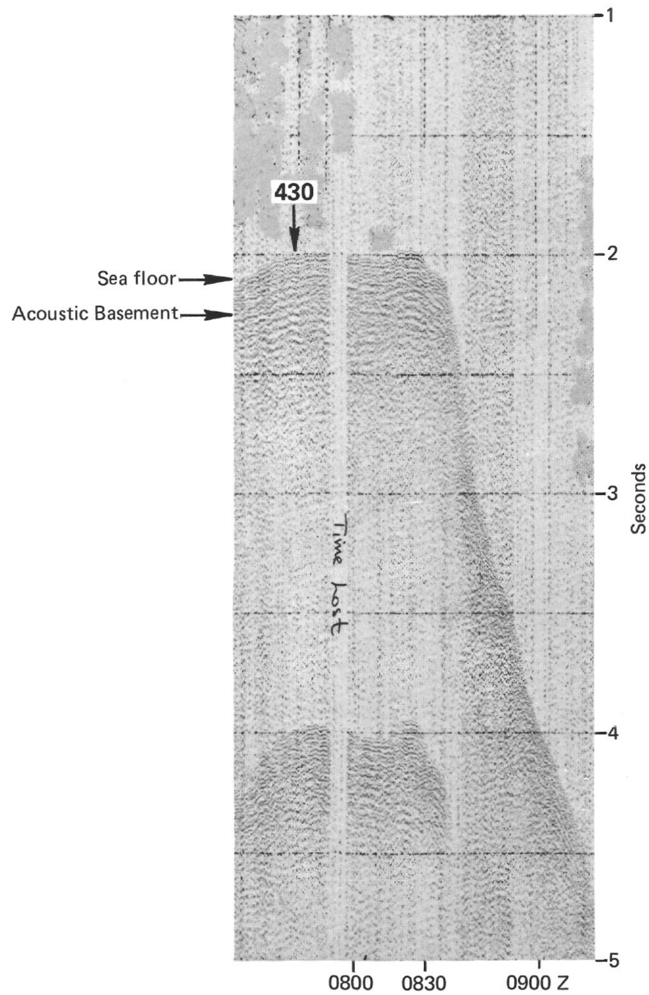

Figure 12. Glomar Challenger *5-s seismic reflection profile on departure from Site 430.*

overlying a shallow, undulating acoustic basement. Apparently, the sediments thin rapidly as the acoustic basement climbs steeply out of the basin to support the seamount's northeastern buttress and bank, and our offset maneuver had placed us over a reduced sediment cover at Hole 430A.

SEDIMENT LITHOSTRATIGRAPHY

Drilling of the sediments on Ōjin Seamount proved difficult. Hole 430 was abandoned because of caving. To achieve a successful entry at Hole 430, the poor consolidation of the sedimentary layers necessitated frequent washing during drilling. The result was minimal sediment recovery, but that recovery was sufficient to determine the stratigraphic sequence on the seamount. The following lithologic units were distinguishable:

Hole	Unit	Lithology	Cores/Samples Represented	Depth below Sea Floor (m)
430	1	Calcareous and volcanic pebbly mud	2; 3, CC	0–14.0
430A	1	Calcareous ooze and sand	1, 2; 3, CC	0–47.5
430A	2	Volcanic ash	4	57.0–59.3

The sediment from Hole 430, Unit 1, contains both calcareous and volcanic components, and has a heterogeneous appearance. The more homogeneous appearance of the sediments from Hole 430A makes them readily separable into two units: calcareous Unit 1 and a predominantly volcanic Unit 2. Deformation of these poorly consolidated sediments during drilling was intense, and obliterated any sedimentary structures that may have existed.

Sediment Description

Hole 430, Unit 1

Recovery for Core 2 was a remarkable 385 per cent. During drilling the material was flushed with water, resulting in an increase in the total amount of sediment recovered and an artificial size separation with depth. Basically, the sediment could be classified as pebbly mud or muddy gravel. It contains both well-rounded and angular clasts of variable origin: brown and red mudstones, red siltstones, weathered basalt, volcanic glass, limestone fragments, calcite-cemented detritus, manganese nodules, and manganese fragments. The pebble size ranges from 0.5 to 2 cm. Texturally, the fine fraction is 55 per cent clay, 30 per cent silt, and 15 per cent sand. Microscopically, the sand is predominantly Mn micronodules (15%), calcareous nannofossils (5%), foraminifers (5%), and quartz (5%). The sediment in this unit is typically very dark grayish brown (10YR 3/2) or dark brown (10YR 3/3).

The only sediment recovered in Core 3 is iron-rich sandstone pebbles found in the core catcher. The sandstones are both fine- and medium-grained, brown (10YR 4/3) and dark yellowish brown (10YR 4/4).

Hole 430A, Unit 1

In Core 1, the upper layer of silty calcareous ooze is very pale brown (10YR 8/4), and contains four altered basalt pebbles (diameter 3 cm) distributed uniformly throughout. In the lower part of the cored section, white, chalky calcareous concretions are mixed with the ooze. Microscopically, the concretions appear to be composed of carbonate (75%) and clay (25%). Two pebbles of nodular limestone were recovered from the core catcher. Macroscopic and thin-section inspection of the pebbles shows that algal nodules and carbonate clasts are cemented with micritic to drusic calcite. The algal nodules themselves are composed of micritized, fibroidal, wavey laminae filled with calcite.

The core-catcher sample of Core 2 also contains the same nodular limestone described for Core 1. The algal nodules are most prominent. Also, volcanic clasts are included in the cemented limestones. The sediment in Core 2 is calcareous sand which contains sand-size pieces of volcanic fragments. The overall color of the sediment is very pale brown (10YR 7/3). Texturally, the finer portion of the sediment is 90 per cent clay and 10 per cent silt. Microscopically, it is composed of clastic carbonate (85%), calcareous nannofossils (10%) and clay 5%). Perhaps the overall sandy texture of the sediment results from the volcanic fragments.

In Core 3, pebbles of calcareous siltstone (yellow 10YR 8/6) and mudstone (dark brown 7.5YR 3/2) were recovered in the core catcher.

Hole 430A, Unit 2

The sediment directly overlying the basaltic flows in Core 430A-4 is silty-sandy ash (dark gray 2.5Y 3/0). Its textural composition is 60 per cent sand, 20 per cent silt, and 20 per cent clay. Microscopically, it contains volcanic fragments (50%), clay (25%), clastic carbonate (15%), feldspar (10%), and heavy minerals (trace amounts). Interspersed in and directly over the dark gray ash are broken fragments of calcarenites composed of fossil debris and ooliths cemented by calcite.

Discussion

Although the amount of sediment recovered at Holes 430 and 430A is limited in quantity, its distinctive character facilitates interpretations of the Eocene environment on Ōjin Seamount. The basalt flows were extruded subaerially, but subsidence below sea level at Hole 430A must have occurred soon after the last flow. The presence of calcarenite fragments in the volcanic ash directly overlying the basalt suggests shallow water. The cemented ooliths in the calcarenite indicate shallow, agitated water. Ooliths are known to form in areas with strong bottom currents, such as tidal bar accumulations or tidal deltas.

Above the volcanic ash zone, calcareous sands and oozes occur in conjunction with nodular limestones. Most of the biogenic calcareous clasts in these sediments are very fine grained, and were probably worked or ground in a high-energy environment. The formation of algal nodules, often called rhodoliths, is restricted to regions within the photic zone and with unstable bottoms where the nodules are occasionally moved by wave action or strong currents. The upward fining of the sediment from calcareous sand to mud reflects a change toward calmer water, possibly representing continued subsidence.

From the seismic profile morphology at Hole 430, it appears that drilling was on a Recent slump. The heterogeneous nature of the recovered material (reef fragments, rounded mudstones, altered basalts, manganese nodules and fragments) at least reveals its multiple origin. The pebbly mud, judging only by its appearance, could have been a near-shore or beach-gravel deposit.

From the sedimentological interpretations of the material cored above the basalt, we conclude that the top of Ōjin Seamount may have been ringed or capped by a reef-lagoonal type of complex during the Eocene. Holes 430 and 430A were drilled at high-energy shallow water sites within this complex. Slow subsidence brought calmer, deeper water. After the Eocene, the seamount continued subsiding, but strong currents in the present water depth have prevented further sedimentation, except for a few centimeters of calcareous sand.

BIOSTRATIGRAPHY

Micropaleontological analyses on board ship were based mainly on examination of core-catcher samples. Continuous coring was planned for all holes at this site, but bottom-hole conditions required some washing in Hole 430A, and the generally poorly lithified sediment cored resulted in low recovery of sediments. Therefore, only rather spotty age identifications and sketchy paleoenvironmental interpretations are possible for the submarine deposits on the platform of Ōjin Seamount at this site.

From 7.7 meters of watery mud and gravel of Core 430-2, moderately preserved calcareous nannofossils of late Eocene date (37–43 m.y.B.P.) were recovered together with fish teeth and echinoidal debris. Although 20 cm of silt and sandstone was collected in Core 430-3, no microfossils were found.

Thin sediments from Cores 430A-1 through 430A-5 directly cap the underlying basaltic rocks of Ōjin Seamount. Calcareous limestone, sandstone, and silt of Cores 430A-1 through 430A-3 yield foraminifers and calcareous nannofossils of late Paleocene to middle Eocene date (43–60 m.y.B.P.). Cores 430A-4 and 430A-5 are transitional between the overlying pelagic sediments and underlying basaltic rocks. Only benthic foraminifers were found, so the ages of sediments remain uncertain. Below Core 5, no microfossils were recovered.

We attempted a punch-core hole (430B) before we left Site 430; but because of what later proved to be a plugged bit, we collected only a very small amount of loose watery sand containing both calcareous (foraminifers and nannofossils) and siliceous (radiolarians, silicoflagellates, and diatoms) Quaternary microfossils.

Foraminifers and Other Microfossils

Hole 430

No sediment was recovered in Core 1, and Core 2 (Sections 1 through 5), the pebbly mudstone, is barren of foraminifers. Some samples from Core 2, however, contain rare echinoids, spines, and fish teeth. Sporadic occurrence of Quaternary planktonic foraminifers in some samples indicates downhole contamination of the cored sediment. Thus, we could assign no age to this sediment on the basis of foraminifers.

Hole 430A

The pale yellowish calcareous ooze and sand of Cores 1 through 3 yielded Paleogene planktonic and benthic foraminifers, together with bryozoa, ostracodes, fish teeth, and calcareous algae and echinoid spines. Planktonic foraminifers are rare to very rare and moderately well preserved to poorly preserved, and show recrystallization of the shells. Some of the stratigraphically diagnostic species in the core-catcher samples (1, CC, 2, CC, and 3, CC) and in other samples (1-1, 30–33 cm; 2-1, 100–102 cm; 2-1, 140–142 cm) include *Globorotalia aequa, G. velascoensis, G. spinulosa, G.* cf. *palmerae, Globigerina linaperta,* and *G. mckannai.* This assemblage suggests that Cores 3 through 1 are upper Paleocene to lower Eocene. During the drilling of Core 4, loose sand (resulting from caving at the hole) was recovered; it was given no section number. This sediment, which may directly overlie the volcanic basement, contains abundant shallow-water biota — such as calcareous benthic foraminifers, bryozoa, ostracodes, gastropods, serpulids, echinoids, and fish teeth — but planktonic foraminifers are absent. In Sample 4-1, 2–13 cm, the sandstone layer overlying the basalt contains shallow-water fauna identical to those mentioned above.

Though benthic foraminifers such as *Cibicides, Lenticulina,* and miliolids at Hole 430A are abundant in all sedimentary cores, they show little diversity and have almost no biostratigraphic resolution.

Hole 430B

The punch-core material collected from Hole 430B consists of Quaternary loose watery sand. Planktonic foraminifers are very abundant, and form the major constituent of the sand fraction of sediment. They are moderately well preserved, indicating their deposition above the dissolution level. Several specimens, however, were damaged in sampling. The assemblage represents the *Globorotalia truncatulinoides* Zone, and includes *Globorotalia truncatulinoides, G. inflata, G. scitula, Globigerina bulloides, G. glutinata, Globigerinoides ruber, Neogloboquadrina dutertrei, N. pachyderma* (dominant right-coiled), and *Orbulina universa.* This assemblage indicates a relatively warm temperature condition corresponding to the present overlying watermass. Benthic foraminifers, on the other hand, are rare, and include *Cassidulina subglobosa, C. lomitensis, C. translucens, Planulina wuellerstorfi, Melonis affinis, Rupertina stabilis, Carpenteria balaniformis, C.* cf. *truncata,* and *Praeglobobulimina spinescens.* The following genera are also occasionally represented in the assemblage: *Fissurina, Oolina, Lagena, Valvulineria, Eponides, Gyroidina, Cassidulinoides, Ehrenbergina,* and *Bolivina.*

Calcareous Nannofossils

Hole 430

No sample was available for Core 1. Core 2 contains a rather poor assemblage, moderately well preserved; identified species include *Dictyococcites bisectus* (most abundant), *Discoaster barbadiensis, D. deflandrei, D. saipanensis, D. tani, Reticulofenestra umbilica, Dictyococcites scrippsae* (common); *Isthmolithus recurvus,* and *Coccolithus eopelagicus* (rare). The occurrences of *Discoaster saipanensis* and *Isthmolithus recurvus,* together with *Discoaster barbadiensis, D. tanii,* and *Reticulofenestra umbilica,* indicate that this sample is upper Eocene (NP 19 *Isthmolithus recurvus* Zone to NP 20 *Sphenolithus pseudoradians* Zone, 37–43 m.y.B.P.). Unless otherwise noted, the chronostratigraphic determinations are based on the standard calcareous nannoplankton zonation proposed by Martini (1971). Because of the general absence of sphenoliths in these samples, further subdivision is impossible at the present time. No calcareous nannofossils were found in Core 3.

Hole 430A

Cores 1 and 2 of Hole 430A contain very limited assemblages, consisting only of *Coccolithus pelagicus* (Cores 1 and 2) and *Cyclicargolithus floridanus* (Core 1 only), together with a small number of tiny placoliths. The preservation is poor to fair, and the ages of these samples cannot be determined. Core 3 contains abundant nannofossils, and the preservation is in general moderately good, except for *Discoaster multiradiatus,* which is in an exceptionally poor state of preservation. The species diversity is low, and the assemblage consists mainly of *Coccolithus pelagicus, Toweius eminens,* and *Neochiastozygus chiastus. Chiasmolithus californicus, Discoaster multiradiatus,* and *Toweius craticulus* are rare. The presence of *Discoaster multiradiatus* and the absence of *Marthasteritus bramlettei* suggest that this sample is probably upper Paleocene and belongs to the NP 9 *Discoaster multiradiatus* Zone (53–60 m.y.B.P.). The remaining samples (Cores 4 through 10) were barren of these nannofossils. Typical shallow-water genera, such as *Braarudosphaera, Micrantholithus,* and *Pemma,* reported from Kōkō Guyot (Sites 308 and 309, Larson, Moberly, et al., 1973), were not represented in the samples studied. However, low species diversity as well as the paucity of nannofossils may result from deposition in a shallow-water environment.

Hole 430B

The moderately well preserved Holocene to upper Pleistocene nannofossil assemblage recovered from Hole 430B consists of *Coccolithus pelagicus* and *Cyclococcolithus leptoporus* (abundant); *Gephyrocapsa oceanica* (common); and *Discolithina japonica, Helicopontosphaera kamptneri,* and *Syracosphaera pulchra* (few to rare). Reworked Miocene and Pliocene specimens such as *Discoaster brouweri, D. exilis, D. variabilis,* and *Cyclicargolithus floridanus* were also recognized. The presence of *Emiliania huxleyi* could not be positively confirmed in the sample studied, because it is too small to identify under the available microscopic equipment, so this sample is tentatively assigned to the NN 20 *Gephyrocapsa oceanica* Zone or the NN 21 *Emiliania huxleyi* Zone (0–0.7 m.y.B.P.).

Radiolarians and Silicoflagellates

Only the sample from Hole 430B contains these siliceous microfossils. They are abundant, well preserved, and of Quaternary age. The assemblage consists of forms commonly found in the surface sediments of present-day mid-latitude transitional region of the North Pacific Ocean. Diatoms are also present in the same sample.

SEDIMENT CHEMISTRY

$CaCO_3$ content of two samples was determined by the carbonate bomb method. Sample 430A-1-1, 89–90 cm, a silty calcareous ooze, contains 86 weight per cent $CaCO_3$; Sample 430A-4-1, 71–72 cm, a mud and ash layer, contains none (Table 3). No interstitial water samples were taken. A sandstone sample was analyzed for density and porosity (Table 4); these results are discussed in the Physical Properties section.

PALEOENVIRONMENT

During late Paleocene to early Eocene time, a reef-lagoonal type of complex developed on the subsiding volcanic island which was to become Ōjin Seamount. At Hole 430A, continued subsidence resulted in a littoral, shallow marine basin with a depth of 5 to 10 meters. High-energy conditions within the basin eroded the reefs and produced coarse-grained sands and calcarenites. Formation of the ooliths and algal nodules cemented in the recovered calcarenites and nodular limestone, respectively, required an unstable bottom with strong wave or current activity. A similar oolitic limestone was found at DSDP Site 202 on Matai Seamount in the South Pacific (Heezen, MacGregor, et al., 1973).

The fossil assemblage of the calcarenites (miliolids, bryozoa, echinoderms, ostracodes, small gastropods and bivalves) indicates shallow marine, lagoonal conditions. With further subsidence, however, the littoral basin became a low-energy neritic environment, as reflected by the change from calcareous sand to calcareous mud. The depth at that time was probably between 10 and 25 meters. The occurrence of some planktonic foraminifers and calcareous nannofossils in the calcareous mud suggests a connection with the open ocean, whereas the presence of benthic foraminifers, such as *Lenticulina* and *Cibicides,* suggests the existence of a shelf-like biota within the subsiding basin.

The pebbly mud facies at Hole 430 may represent a shoreline deposit. Most of the pebbles are well rounded, probably because of intense wave activity in a near-shore environment. Echinoidal spines and fish teeth are the only biogenic elements found in this sedimentary unit. The shoreline facies at Hole 430 and the basinal facies at Hole 430A may be interpreted as two lithological units having a lateral facies relation. The morphological features at the site of the pebbly mud probably represent slumping of the sedimentary material on the sloping sides of the ancient basin.

The upper Eocene to Pliocene stratigraphic record is missing at Holes 430 and 430A. This is apparently a result of effective erosion and scour by currents during the subsidence history of the seamount. The Quaternary unconsolidated watery sand obtained at Hole 430B suggests present-day pelagic sedimentation on the rocky submerged areas of the seamount. Current activity still prevents accumulation of fine-grained pelagic material on the seamount. The planktonic microfaunal and microfloral assemblages in the Quaternary sand reflect a temperate oceanic environment for the overlying water-mass. The good preservation of these calcareous fossils indicates that the top of Ōjin Seamount is above the present carbonate compensation depth (CCD).

LITHOSTRATIGRAPHY OF VOLCANIC ROCKS (HOLE 430A)

At Hole 430A we recovered portions of five different volcanic flow units in the interval from Section 4-2 (83 cm) to Section 6-4, Piece 18 (150 cm). Figure 13 illustrates the recovery in this interval and the position of the flow boundaries. The top four of these units consist of similar, nearly aphyric, basalt, and one (represented by only two pieces near the bottom of Core 6) consists of plagioclase and pyroxene phyric basalt.

The boundaries between Flow Units 1 and 2 and between Units 2 and 3 are determined mainly by changes in color and vesicularity. The tops of Flow Units 2 and 3 are highly vesicular, whereas the bottoms of these flows are massive. Vesicles in flow tops are open, but the few vesicles present in the more massive bases are filled with

TABLE 3
$CaCO_3$ Analyses, Carbonate Bomb Method, Hole 430A

Core	Section	Interval (cm)	$CaCO_3$ (%)
1	1	89-90	86
4	1	71-72	0

TABLE 4
Water Content/Bulk Density/Porosity of Sediments

Core	Section	Interval (cm)	Water Content (%)	Porosity (%)	Wet-Bulk Density (g/cm^3)
4	1	44-46	12.4	28.7	2.32

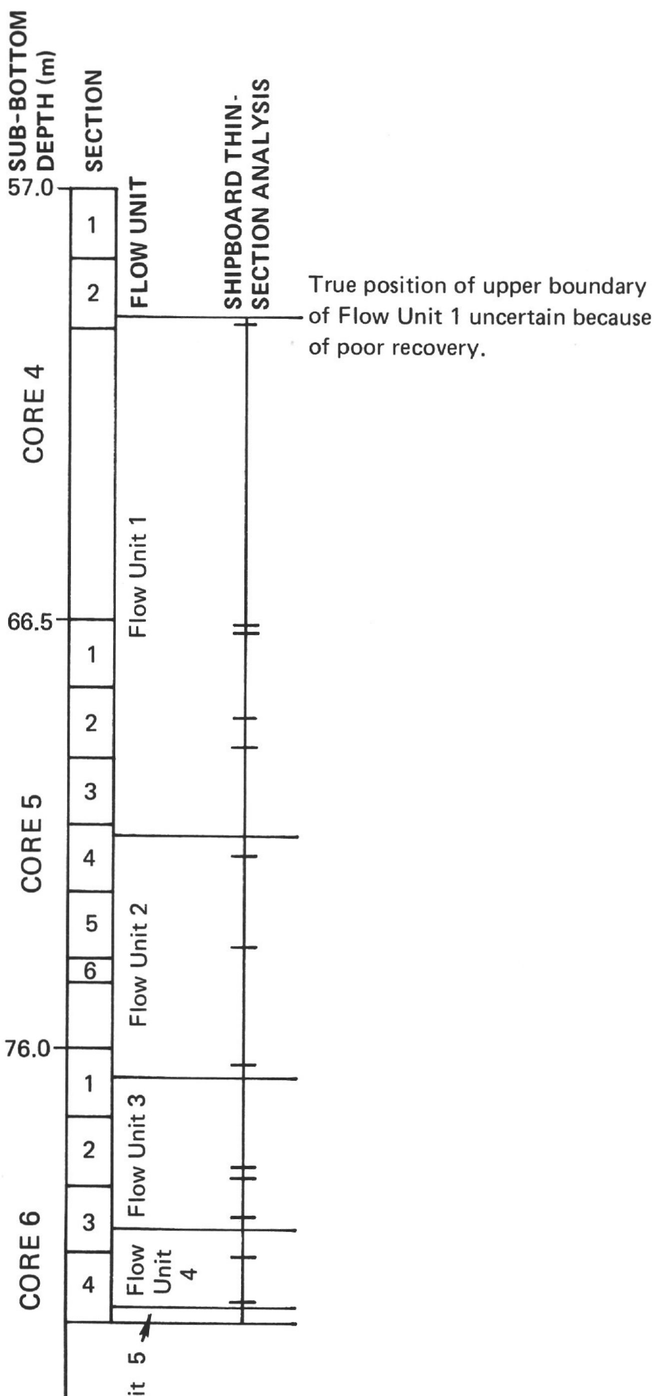

Figure 13. *Recovered portions of five basaltic flow units and the positions of the flow boundaries.*

calcite and green clays. Flow Unit 3 is underlain by a red soil horizon, at the base of Section 6-3, which marks the base of the flow unit. The rocks in Section 6-4 (which was recovered from the bit) and in the core-catcher samples from Cores 10 and 11 may be grouped into two discrete groups. Pieces 14 and 18 of Section 6-4 are highly porphyritic, whereas the rest of the rocks are aphyric. The samples from Section 6-4 and the core-catcher samples have been designated as Flow Units 4 and 5, on the basis of abundance of phenocrysts. The aphyric flow unit overlies the porphyritic flow, since one long (about 20 cm) oriented piece of aphyric basalt was recovered from the top of the bit and the largest porphyritic piece was the lowest piece in the bit.

Flow Unit 1 extends from Section 4-2 (82 cm) to Section 5-4 (Piece 1d, 31 cm). The flow is aphyric and directly overlain by a volcaniclastic sandstone. The topmost piece has a pelecypod shell attached, indicating that the flow was essentially at sea level when sediment accumulation started. Near the top, the flow is slightly altered, but most is dark gray and appears very fresh in hand specimen. The groundmass (0.1 mm) consists of plagioclase, pyroxene, and rare olivine. Single phenocrysts of altered olivine and feldspar are visible in the core. The top few pieces in Section 4-2 contain a few 1-mm vesicles, some of which are calcite and clay filled or lined. The bottom of the unit in Section 5-4 contains elongated vesicles and vugs filled with calcite and clay. The rest of the unit is very dense, and contains only a few vesicles, mostly filled with calcite. Thin bands that may be altered glass in Section 5-1 (Pieces 3A and 11) are probably segregation veins or glass selvages incorporated in the flow as it cooled. We have not interpreted these as flow unit boundaries. Several nearly horizontal veins are filled with calcite.

Flow Unit 2, which extends from Section 5-4 (Piece 2) to Section 1 (Piece 8), also consists of nearly aphyric basalt, although there are altered olivine microphenocrysts (3 to 4%) near the top. The groundmass is fine grained, and consists of about 60 per cent plagioclase, 30 per cent pyroxene plus dark alteration material, and 10 per cent altered olivine. The top of the flow from Section 5-4 (Piece 2) to Section 5-5 (Piece 5) contains about 20 to 30 per cent vesicles which average about 5 mm in diameter. Some are filled with calcite. Most of those not completely filled are lined with botryoidal green or smooth brown clay. From Section 5-5 (Piece 6) to Section 5-6 (Piece 1), the vesicles become smaller and are mostly filled with clay and, more rarely, calcite. Below this horizon the rock has few vesicles, except near the very bottom, where about 10 per cent of the rock is made up of vesicles filled with green clay and calcite. In the vesicular top of the flow, the rock is moderately altered to a brownish gray color. The massive part of the flow is dark gray and appears fresh, although in the darker mottled areas the groundmass is probably altered.

Flow Unit 3 extends from Section 6-1 (Piece 9) to Section 3 (Piece 8), and consists of aphyric basalt similar in appearance to Flow Unit 2. The groundmass is 50 per cent plagioclase, 40 per cent pyroxene plus dark alteration materials, and 10 per cent moderately altered olivine. From the top of the flow to Section 6-2 (Piece 7), the rock is moderately altered to a brownish green color, and contains about 30 per cent vesicles, 5 to 7 mm in diameter, lined with green clays. In Section 2, from Piece 8 to Piece 10, the vesicles become progressively smaller and less abundant and more completely filled with green clay and calcite. From Section 2 (Piece 1) to the bottom of the flow unit, the basalt is dark gray and massive, with only a few vesicles filled with calcite, and appears fresh, although, as in Flow Unit 2, the dark mottled material is altered groundmass.

The material in Section 6-3 (Piece 9) is moderately to extensively altered basalt with some reddish soil that probably represents a soil horizon developed on the top of a flow unit stratigraphically beneath Flow Unit 3.

The material archived as Section 6-4 was recovered in the bit when the pipe was finally pulled. It probably fell into the bit when Core 6 was pulled, since recovery stopped after this core. The pieces in this section are probably not in correct stratigraphic sequence. Assuming that the altered material in Section 3 (Piece 9) is in its correct stratigraphic position, Section 4 contains rock from two flow units. Most of the pieces (1 through 13 and 14 through 17) are dense, dark gray aphyric basalt very similar to the dense parts of Flow Units 1, 2, and 3. We have called this material Flow Unit 4.

Pieces 14 and 18 are from a different flow unit, which we have designated as Unit 5. The rock is porphyritic, with 15 to 20 per cent phenocrysts or glomoeroporphyritic clots (up to 3 mm in diameter) of intergrown plagioclase and pyroxene; some of the clots appear rounded. The groundmass is fine grained, and is composed of 70 per cent plagioclase, 25 per cent pyroxene, and 5 per cent altered olivine. The rock contains a few 1- to 2-mm vesicles filled with green clay.

The few pieces recovered in Cores 10 and 11 are probably from the Core 6 material dropped in the bit, and are here designated part of Flow Unit 4.

PETROGRAPHY OF VOLCANIC ROCKS (HOLE 430A)

Flow Unit 1

The top of Flow Unit 1 was not recovered, probably because it had been eroded away when the seamount was at sea level. This conclusion is based on the weathered and fractured appearance of the topmost recovered lava, the angle between the top of the flow unit and the core, and the presence of a large attached pelecypod on the surface. The entire flow is massive, although a few filled vesicles appear near the bottom of the flow. A thin section was made from each of five samples from Flow Unit 1: Samples 4-2, 115–116 cm; 5-1, 5-7 cm; 5-1, 16–19 cm; 5-2 84–86 cm, and 5-2, 120–123 cm. No thin sections were made from the base of the unit, because of the filled vesicles and because the core appears to be highly altered.

The entire flow is aphyric, and the feldspars are fairly well aligned horizontally, giving the rock a subtrachytic texture. Near the top of the flow the groundmass is intersertal, but from Sample 5-1, 5–7 cm downward the clinopyroxene is subophitic to ophitic. Pyroxene grain size increases from 0.1 mm near the top of the flow to 0.9 mm near the middle of the flow unit. The average grain size for all phases is about 0.2 to 0.3 mm for the entire flow.

The flow contains rare phenocrysts of mostly iddingsitized olivine, resorbed plagioclase (about An_{55} in the unzoned cores), and less than 1 per cent microphenocrysts of plagioclase and titanomagnetite. The groundmass is composed of about 60 per cent felty plagioclase laths ($\sim An_{30-35}$?), 10 to 20 per cent titanomagnetite, 5 per cent totally altered olivine, and 25 per cent combined clinopyroxene and clay secondary after interstitial glass. Near the top of the flow there is only 1 to 3 per cent clinopyroxene and 25 per cent clay, but farther into the flow the proportion of clinopyroxene increases to nearly 15 per cent and the clay content decreases to about 10 per cent. Apatite is fairly abundant, and occurs both as long (0.1 to 0.2 mm) acicular needles and as stumpy hexagonal crystals. The olivine is altered to iddingsite near the top of the flow and to fibrous green clay (saponite) toward the flow center. Plagioclase is fresh except in the upper part of the flow (Sample 4-2, 115–116 cm) where some plagioclase is replaced by clays.

The titanomagnetite is extremely fresh in all thin sections except that from Sample 4-2, 115–116 cm, where some of the titanomagnetite has exsolved and altered to magnetite and an unidentified dark gray phase (pseudobrookite?). In Sample 5-1, 5–7 cm, most of the titanomagnetite has exsolved to ilmenite plus titanomagnetite or, in rare cases, magnetite. The amount of exsolution decreases down the section until the titanomagnetite is exsolved in Sample 5-2, 120–123 cm.

The clinopyroxene is extremely fresh and very pale brown. Optical determination of pyroxene compositions is difficult and somewhat unreliable, owing to the large number of possible substitutions into the pyroxene lattice, but the high $2V^+$ ($\sim 60°$) indicates a high-Ca clinopyroxene, probably salite or diopside.

The interstitial glass is completely replaced by greenish yellow to brown clays, which gives the rock a rather muddy appearance in thin section. Where apatite grains are enclosed by clays, they are surrounded by a darkened zone similar in appearance to the pleochroic halos that form around apatite set in biotite. Clays also fill the extremely rare vesicles in the upper 4/5 of the flow and the more abundant ($\sim 10\%$) vesicles in the lower part of the flow.

Flow Unit 2

Flow Unit 2 has a very vesicular top that grades downward to a massive portion of the flow. One thin section taken from the vesicular upper part of the flow (Sample 5-4, 52–65 cm) and two from the massive part of the flow (Sample 5-5, 126–128 cm and Sample 6-1, 33–35 cm).

This flow unit is very similar to Flow Unit 1. The rock is nearly aphyric, with very rare phenocrysts of resorbed plagioclase and equant titanomagnetite. The plagioclase laths are well aligned, giving the rock a trachytic to subtrachytic texture. Plagioclase is mostly fresh; some minor alteration of clays has occurred along fractures. Near the flow top the proportion of vesicles (to 10 mm) is 20 to 25 per cent; near the center the flow is massive. There are vesicles (about 5%) filled with clay and calcite near the base of the flow. The clinopyroxene in the massive part of the flow is ophitic to subophitic; near the top of the flow it is intergranular. Most of the clays replace interstitial glass. The average grain size is about 0.1 to 0.2 mm, and is fairly constant throughout the flow.

The clinopyroxene is colorless to very pale brown, and increases in abundance from 5 per cent near the top of the flow to nearly 15 per cent near the bottom. As the percentage of clinopyroxene increases, the texture grades from intersertal to nearly ophitic, with single plates of pyroxene up to 0.3 mm. The proportion of clays is inversely proportional to the percentage of pyroxene.

The opaque oxides consist of titanomagnetite and, in abundance near the flow top, its exsolution products ilmenite and magnetite; only rare exsolution has occurred near the base. Some alteration of the titanomagnetite to an unidentified dark gray phase (pseudobrookite?) has occurred in the topmost sample.

Flow Unit 3

Flow Unit 3 is nearly identical to Flow Unit 2. The flow is highly vesicular near the top and grades downward into a massive lava. The base of the flow was probably not recovered, although a red soil horizon suggests that the bottom of Section 6-3 is a flow boundary.

Three thin sections were made from Flow Unit 3, all from Samples taken in the massive part of the flow: 6-2, 102–105 cm; 6-2, 134–136 cm; and 6-3, 68–70 cm. The vesicular top of the flow was not sampled, because of the prevalence of vesicle infilling by clays and calcite.

The flow is nearly aphyric, having only two microphenocrysts of resorbed plagioclase in all three thin sections. The feldspar laths are quite strongly aligned with a sub-horizontal orientation, and give the rocks a subtrachytic texture. The groundmass is intersertal, although the interstitial glass is now entirely altered. The average grain size is about 0.1 to 0.2 mm.

The groundmass is composed of about 58 per cent plagioclase laths, 0 to 3 per cent altered olivine, 9 per cent titanomagnetite, 2 to 15 per cent clinopyroxene, and 1 per cent apatite. The remainder is interstitial glass altered to clay. Near the top of the flow, but within the massive portion, there is only 2 per cent clinopyroxene; down-core the percentage of clinopyroxene increases to nearly 15. As clinopyroxene becomes more abundant, the percentage of clays replacing interstitial glass decreases and the texture of the groundmass becomes subophitic.

In thin sections prepared from Samples 6-2, 102–105 cm and 6-2, 134–136 cm, the titanomagnetite is extensively exsolved to ilmenite, magnetite, and titanomagnetite. There is also some alteration of the titanomagnetite to an unidentified dark gray phase (pseudobrookite?). In a thin section from Sample 6-3, 68–70 cm, the titanomagnetite is unaltered, but is partly exsolved to ilmenite and magnetite. Some of the elongate groundmass grains are magnetite.

As in Flow Units 1 and 2, the large percentage of clays replacing interstitial glass gives the rocks a muddy appearance.

Flow Unit 4

Specimens from Flow Unit 4 were recovered in the core-catcher samples of Cores 10 and 11, and from the bit when it was brought on deck. We believe that these basalt pieces are from the bottom of Core 6, and the bit recovery is so labeled (Section 6-4). Stratigraphically, Samples 10, CC and 11, CC *overlie* Section 6-4.

Thin sections were cut from three samples in Flow Unit 4. The samples are, from top to bottom, 10, CC (28–30 cm), 11, CC (Piece 1), and 6-4 (0–1 cm). These three samples are petrographically similar and are distinct from the rocks sampled in Flow Units 1 to 3. The flow boundary between Flows 3 and 4, first identified by the presence of a soil horizon, is substantiated by the thin sections, since the rocks above and below are different.

The samples from Flow Unit 4 are nearly aphyric, with very rare microphenocrysts of plagioclase and titanomagnetite. The feldspar laths are subparallel, with a horizontal orientation, and give the rock a subtrachytic texture. Some of the pieces recovered in Section 6-4 (the bit recovery) are platy in hand specimen, suggesting strong flow orientation of the feldspars. The average grain size is 0.05 mm.

The groundmass is composed of 50 to 60 per cent plagioclase (An_{30-35}), 10 to 15 per cent clinopyroxene, 5 per cent titanomagnetite, 1 to 2 per cent apatite, 2 to 5 per cent olivine, and the remainder is clay secondary after interstitial glass. The plagioclase laths are as long as 0.5 mm, and are beginning to alter to clays along fractures. The clinopyroxene is colorless and generally intergranular. The olivine is mostly altered to greenish fibrous clays (saponite), but fresh cores (Fo_{65}) are common. The presence of olivine distinguishes Flow Unit 4 from Flow Units 1 to 3. The titanomagnetite is totally fresh, and is only rarely exsolved to ilmenite and titanomagnetite or to ilmenite and magnetite. The greenish clays replace mostly intersertal glass and the rims of olivine grains.

Flow Unit 5

Flow Unit 5 was recovered from the bit and is part of Section 6-4. Only two small pieces were recovered, and no thin section was made. The rock is moderately porphyritic (15%) and has glomerocrysts of plagioclase and pyroxene.

Comparison of Flows

The top four flow units are petrographically similar. Each flow has abundant plagioclase and a trachytic to subtrachytic texture. In each of the three flows with good recovery, the percentage of clinopyroxene increases toward the base of the flow and the percentage of clays replacing glass decreases. In each flow, as the percentage of clinopyroxene increases downflow, the texture grades from intersertal to subophitic to ophitic. In each flow, the sequence of crystallization is microphenocrysts of olivine, plagioclase, and titanomagnetite, followed by plagioclase and apatite, then, in order, titanomagnetite, clinopyroxene, and interstitial glass.

The titanomagnetite in each flow is partly altered near the flow tops, but is totally fresh in the interiors. It is extensively exsolved near the flow tops, and nearly exsolved toward the flow bases.

Flow Unit 4 contains some olivine that still has fresh cores, a feature not shared by Flow Units 1 to 3.

Flow Unit 5, although not thin-sectioned, is quite distinct from the overlying four flow units, in that it is a porphyritic basalt.

Classification

Flow Units 1 to 4 are nearly identical, and are highly differentiated lava. The abundant sodic plagioclase (An_{30-35}) and relatively fayalitic olivine (Fo_{65}) indicate that the flows are approximately hawaiite in composition. The thicknesses of the flows, the massive nature of the flow interiors, the nearly conchoidal fracture of the rocks, and the subtrachytic texture are all compatible with this classification. The abundance of apatite is a further indication of the alkalic nature of these lavas. The abundant ophitic clinopyroxene is unusual in Hawaiian rocks of this composition, and in addition the flows are generally coarser grained than their Hawaiian counterparts.

No shipboard thin section was made of Flow Unit 5, but petrographic and chemical data obtained subsequently show that it is a tholeiitic basalt.

CHEMISTRY OF VOLCANIC ROCKS (HOLE 430A)

Thirteen samples from Hole 430A on Ōjin Seamount were analyzed aboard ship, using analytical methods outlined by Bougault et al. (1977) and in the XRF procedures chapter of the Leg 46 shipboard reports.

Twelve of the analyzed samples are from volcanic flows, and the thirteenth is from the volcanic sandstone overlying volcanic Flow Unit 1. The 12 flow samples include samples from each of the five cored flow units: four samples from Flow Unit 1, two from Flow Unit 2, three from Flow Unit 3, two from Flow Unit 4, and one from Flow Unit 5. The shipboard analyses, dry reduced analyses, and norms assuming $Fe^{+3}/(Fe^{+3} + Fe^{+2}) = 0.15$ are listed in Table 5. Figure 14 is a plot of total alkalis versus silica.

The samples from Flow Units 1 through 4 are chemically very similar, though not identical. Table 6 lists a mean analysis for each flow. In particular, the TiO_2 concentration varies very slightly among the top four flows; the variations are greater than the analytic precision and the intraflow variations, and we believe they reflect interflow variation. Flow Unit 5 is clearly different from Flow Units 1 through 4.

Flow Units 1 through 4 are strongly alkalic, as shown by the K_2O and P_2O_5 values, and also strongly differentiated, as shown by the low percentages of MgO and CaO and the high percentage of Fe_2O_3. Comparison of the cored lavas with average Hawaiian lavas (Table 7) suggests that the lavas cored in Flow Units 1 through 4 are similar to hawaiite, although the cored lavas are distinctly high in P_2O_5 content.

Flow Unit 5 is not like any of the average Hawaiian rock types calculated by Macdonald (1968). The low K_2O and P_2O_5 contents and the unit's position in the plot of total alkalis versus silica (Figure 14) indicate that the lava is a tholeiitic basalt of the oceanic island type. The lower than average SiO_2 content and higher than average concentrations of Al_2O_3 and CaO are probably caused by the abundant plagioclase phenocrysts the lava contains. The MgO concentration is low for a tholeiitic basalt; this probably results from fractionation of olivine.

Island-type tholeiite is an unusual rock type on intraplate volcanoes. In the Pacific basin, island tholeiite is known only from a few seamounts that formed near the mid-ocean ridge, from the volcanoes that make the Hawaiian Islands (Macdonald, 1968), the Hawaiian Ridge (Clague, 1974; Dalrymple et al., 1974; Macdonald, 1969), and from Kōkō and Diakakuji seamounts in the southern Emperor Seamount chain (Clague, 1974; Clague et al., 1975). Recovery of an island tholeiite from Ōjin Seamount provides further evidence that the Emperor Seamounts are volcanoes of the Hawaiian type, and that the Emperor Seamounts and Hawaiian Ridge are genetically related.

Stearns (1946a, b) and Macdonald (1968) have stressed that petrologically distinct lavas erupt during different stages of development of a Hawaiian volcano. The lavas of the main shield-building stage, which erupt very rapidly and in great volume, are tholeiitic basalts, and only minor alkalic or transitional lavas erupt during the waning stages of shield-building. The shield-building phase is followed by caldera collapse and the eruption of a thin veneer of alkalic basalts and associated differentiated lavas. Finally, after as much as 4 m.y. of quiescence, alkalic basalts and strongly undersaturated lavas may erupt from satellite vents.

Applying this eruptive sequence from the Hawaiian Islands to the drilled basalts, we conclude that the tholeiitic basalt represents the shield-building stage of volcanism, and that the hawaiites probably represent volcanism during the alkalic stage which follows caldera collapse.

In the Hawaiian Islands, the alkalic and post-erosion lavas generally form a thin veneer on the top of the volcano. If Ōjin Seamount had only a similar veneer of alkalic lava, it seems probable that it would have eroded away during the period of erosion when the nearly flat top of the seamount formed. It is possible that the alkalic flows were very thick, as on Waianae volcano on Oahu, or that the hawaiites recovered were erupted after the top of the volcano was eroded flat by wave action. In this latter case, these lavas would have to be considered post-erosional. Until more detailed chemical and mineralogical studies are completed, the eruptive stage of the hawaiite is uncertain, although eruption during an alkalic stage seems most probable.

TABLE 5
Analyses of Volcanic Samples, Hole 430A

Core/Section/Piece No.	4-1	4-2	5-1, #1	5-1, #2A	5-2, #6C	5-5, #10D	6-1, #2B	6-2, #10	6-2, #13	6-3, #6	10, #CC	6-4, #18
Interval (cm)	68-70	139-142	5-7	16-19	120-123	127-129	33-35	102-105	133-136	68-70	28-30	143-146
Rock Type	Volcanic sandstone	Hawai-ite	Hawai-ite	Hawai-ite	Hawai-ite	Hawai-ite	Hawai-ite	Hawai-ite	Hawai-ite	Hawai-ite	Hawai-ite	Tholeiitic Basalt
Lithologic Unit		Flow 1	Flow 1	Flow 1	Flow 1	Flow 2	Flow 2	Flow 3	Flow 3	Flow 3	Flow 4	Flow 5
Major-Element Oxides (wt. %)												
SiO_2	49.77	49.03	49.96	49.10	49.50	49.81	49.60	49.29	49.80	50.02	49.63	48.38
TiO_2	2.93	3.16	3.13	3.13	3.00	3.03	3.02	2.88	2.87	2.90	2.86	2.79
Al_2O_3	15.16	15.96	16.09	16.17	15.57	15.84	15.72	15.99	15.98	16.05	15.76	15.44
Fe_2O_3 (Total)	14.04	13.02	12.41	13.28	12.87	12.22	12.31	12.39	12.00	11.72	12.46	13.07
MnO	0.07	0.09	0.08	0.09	0.13	0.10	0.11	0.13	0.12	0.12	0.14	0.18
MgO	6.87	3.78	3.73	3.09	4.78	4.31	4.12	4.74	4.76	4.11	4.71	5.41
CaO	3.41	6.96	7.01	7.17	6.95	7.24	7.18	6.85	7.02	7.02	6.99	11.05
Na_2O	4.10	4.30	4.40	4.20	4.10	4.20	4.10	4.40	4.20	4.30	4.00	2.80
K_2O	2.67	1.85	1.79	1.77	1.60	1.66	1.66	1.68	1.73	1.73	1.70	0.36
P_2O_5	0.35	1.27	1.26	1.25	1.19	1.31	1.27	1.35	1.36	1.32	1.29	0.33
Total	99.37	99.42	99.66	99.25	99.69	99.72	99.09	99.70	99.84	99.29	99.54	99.81
Loss on Ignition (wt. %)	25.77	4.26	4.16	4.44	3.15	3.61	3.29	3.81	3.55	3.20	2.82	1.08
H_2O^+ wt. % Composition	2.69	1.04	0.89	0.91	1.59	1.45	1.34	1.67	1.54	1.41	1.55	0.38
CO_2 after baking off H_2O	0.15	0.15	0.04	0.18	0.03	0.05	0.07	0.07	0.06	0.07	0.05	0.03
Mg/(Mg + Fe)	0.49	0.37	0.37	0.32	0.42	0.41	0.40	0.43	0.44	0.41	0.43	0.45
Trace Elements (ppm)												
Ni		20	19	18	18	15	15	15	14	14	12	58
Sr		680	676	675	640	660	645	627	652	662	664	423
Zr		459	458	452	446	478	458	459	469	466	470	169

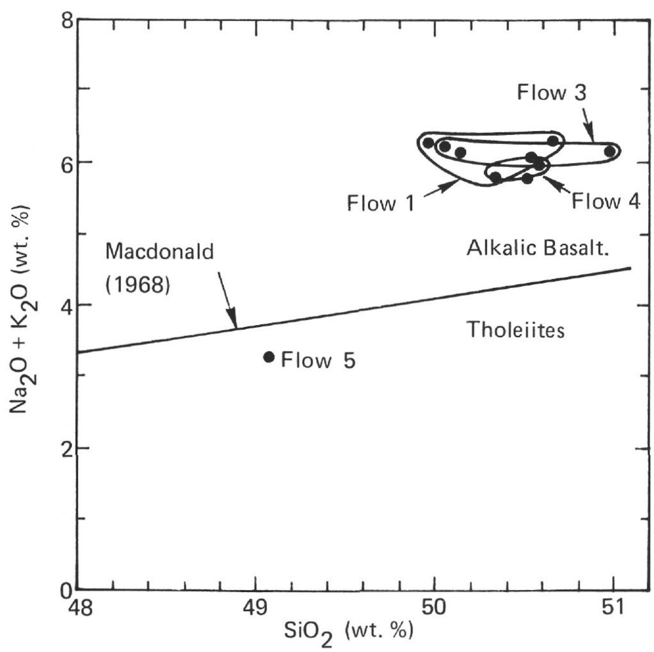

Figure 14. *Total alkalis versus silica for Site 430 basalts.*

TABLE 6
Average Chemical Analyses of Volcanic Rocks from Hole 430A, Ōjin Seamount

Major-Element Oxides (wt. %)	Flow 1	Flow 2	Flow 3	Flow 4	Flows 1-4	Flow 5
SiO_2 (wt. %)	49.40	49.70	49.70	49.60	49.60	48.38
TiO_2	3.10	3.02	2.88	2.84	2.96	2.79
Al_2O_3	15.87	15.78	16.01	15.76	15.86	15.44
Fe_2O_3 (Total)	12.90	12.26	12.04	12.40	12.40	13.07
MnO	0.10	0.10	0.12	0.14	0.12	0.18
MgO	3.84	4.22	4.54	4.64	4.31	5.41
CaO	7.02	7.21	6.96	6.90	7.02	11.05
Na_2O	4.25	4.15	4.30	4.00	4.18	2.80
K_2O	1.75	1.66	1.71	1.71	1.71	0.36
P_2O_5	1.24	1.29	1.34	1.28	1.29	0.33
Total	99.51	99.41	99.61	99.54	99.52	99.81
Loss on Ignition (wt. %)	4.00	3.45	3.52	3.18	3.54	1.08
Mg/(Mg + Fe)	0.37	0.40	0.42	0.42	0.40	0.45
Trace Elements (ppm)						
Ni	19	15	14	14	16	58
Sr	668	652	647	646	653	423
Zr	454	468	465	464	463	169

PALEOMAGNETISM

Introduction

Leg 55 was planned to test the applicability of the hot-spot hypothesis to the origin of the Emperor Seamount chain. The main objective of the shipboard paleomagnetic study was therefore to establish the paleolatitudes of the seamounts from the inclination of the natural remanent magnetization (NRM) in basaltic layers forming these seamounts. To do so, extensive sampling and measurements of basalts was planned. In addition, a limited effort was directed to study the NRM directions in sedimentary layers overlying basement.

Estimation of Paleolatitudes

The present geomagnetic field is well approximated by a field produced by a dipole located at the earth's center and tilted 11.5° from the rotational axis. Paleomagnetic studies have shown that the dipolar nature of the magnetic field has persisted for the periods of Quaternary and late Tertiary where the effect of horizontal movements of landmasses may be neglected, and that

TABLE 7
Average Compositions of Hawaiian Lavas (wt. %)[a]

Type of Rock	Tholeiitic Suite		Alkalic Suite							Nephelinic Suite					
	Oceanite	Tholeiite and Olivine Tholeiite	Ankaramite	Alkalic Olivine Basalt	Feldspar-Phyric Basalt	Hawaiite	Mugearite	Benmoreite	Soda Trachyte	Alkalic Olivine Basalt (basanitoid)	Basanite	Mimosite	Nephelinite	Ankaratrite	Melilite Nephelinite
Number of Analyses	14	200	9	35	6	62	23	5	5	11	11	4	10	1	7
SiO_2	46.4	49.4	44.1	45.4	46.6	47.9	51.6	57.1	61.7	44.8	44.1	41.3	39.7	39.4	36.6
Al_2O_3	8.5	13.9	12.1	14.7	16.8	15.9	16.9	17.6	18.0	12.7	12.7	10.4	11.4	10.2	10.8
Fe_2O_3	2.5	3.0	3.2	4.1	4.5	4.9	4.2	4.8	3.3	3.2	3.6	5.6	5.3	6.5	5.7
FeO	9.8	8.5	9.6	9.2	8.1	7.6	6.1	3.0	1.5	9.4	9.1	8.3	8.2	7.0	8.9
MgO	20.8	8.4	13.0	7.8	5.8	4.8	3.3	1.6	0.4	11.4	11.2	13.8	12.1	14.1	12.6
CaO	7.4	10.3	11.5	10.5	9.3	8.0	6.1	3.5	1.2	11.4	10.6	12.1	12.8	12.3	13.6
Na_2O	1.6	2.2	1.9	3.0	3.2	4.2	5.4	5.9	7.4	2.7	3.6	2.8	3.8	2.7	4.1
K_2O	0.3	0.4	0.7	1.0	0.8	1.5	2.1	2.8	4.2	0.9	1.0	0.9	1.2	1.2	1.0
TiO_2	2.0	2.5	2.7	3.0	3.3	3.4	2.4	1.2	0.5	2.3	2.6	2.7	2.8	3.3	2.8
P_2O_5	0.2	0.3	0.3	0.4	0.4	0.7	1.1	0.7	0.2	0.5	0.5	0.7	0.9	0.8	1.1
MnO	0.2	0.2	0.2	0.2	0.2	0.2	0.2	0.2	0.2	0.2	0.2	0.2	0.2	0.1	0.1
$FeO:Fe_2O_3$	4.0	2.8	3.0	2.2	1.8	1.6	1.4	0.6	0.4	2.9	2.5	1.5	1.5	1.1	1.6

[a]From Macdonald, 1968.

the magnetic field direction at a site averaged over a suitable time interval is close to the field directions expected from an axial centered dipole. Magnetic inclination I is therefore related to paleolatitude θ as

$$\frac{1}{2}\tan I = \tan \theta$$

and the paleolatitude of a site can be determined from measurements of NRM in rocks, using the above equation. There are, however, several factors which may cause errors in estimating paleolatitudes. We shall now briefly consider each of them.

Experimental Error

This includes errors in the orientation of rock samples, and those in the measurement of NRM directions. Paleomagnetic samples are taken from the drilled core assuming that the core axis was vertical. Drilling experts estimate the error involved in this assumption to be less than a few degrees. Drilling minicores for paleomagnetism is done very carefully, and the orientation error in this stage may be typically about one degree, although in a few cases an error of about three degrees has been caused by inadequate cutting of the core segments into halves.

The reproducibility of a measurement was estimated from repeated measurements of a standard sample to be about 0.5 degree for rocks with magnetism larger than 10^{-4} emu/cm³ (10^{-1} A/M). The error in this category (except the verticality of the drilled core) is random and can be eliminated by averaging over multiple samples from the same cooling unit.

Local Anomalies, Random

Strongly magnetized rock bodies can appreciably deform the local magnetic field and cause strong local anomalies. These deflections of magnetic directions are more pronounced at the edges of the magnetized bodies. It is not very uncommon to observe differences of about 10° in NRM directions measured on separate samples from a single lava flow. Measurements on recent lavas show that such deflections are random, so that they can be averaged out by the use of multiple samples, appropriately spaced.

When a rock formation is tilted, the stable remanence in the rock is likewise tilted. The field direction can be recovered by tilt correction, which means to rotate the formation back to its original (usually horizontal) position. In a drill core, it is very difficult to assess the possible tilt of lava flows. However, since the drilling sites are selected on the basis of good, continuous basement reflectors and an undisturbed sedimentary layer above that on seismic profiles, we may not be in great error by assuming that the cores were taken from undeformed strata.

Secondary Magnetization

In volcanic rocks or sediments the primary component of magnetization is acquired when the rock is formed, either as thermoremanent magnetization (TRM) or as detrital remanent magnetization (DRM). The rocks may also have subsequently acquired secondary components of magnetization, and the primary component may have spontaneously decayed, so that the NRM observed may be considerably different from the original remanence.

The spontaneous decay of remanence is a serious problem in studies of paleomagnetic intensity, but it does not affect the direction of remanence. Secondary components of magnetization are acquired mostly by one of the mechanisms discussed below.

Isothermal remanent magnetization (IRM) is magnetization acquired by a sample when it is placed in a strong magnetic field for a short time. IRM is often observed in rocks which received lightning strikes. In such rocks the direction and intensity of magnetization is greatly scattered, making the effect easy to recognize. IRM is also a soft magnetization, and is easily demagnetized by a 100 to 200 Oe (10 to 20 MT) alternating field.

When a rock is placed in a magnetic field for a long period of time, it acquires viscous remanent magnetization (VRM), the stability of which increases with the acquisition time. As the magnetic viscosity effects work equally on production of VRM and decay of other remanences, it is sufficient to consider the effect of VRM acquired in the last constant polarity period, i.e., Brunhes normal epoch. When the direction of the primary component is different from the present axial dipole field directions, the presence of VRM can be shown by stepwise alternating-field (AF) demagnetization; remanence direction moves on a great circle path connecting the two field directions.

When chemical changes take place below the Curie temperature of their ferromagnetic minerals, rocks may acquire chemical remanent magnetization (CRM). In sub-oceanic basalts, ferromagnetic minerals are often found to have been partially or totally oxidized to titanomaghemites. The effect of this low-temperature oxidation on NRM is still not very clear, but it is presumed that the primary component is not totally destroyed, although the intensity and stability of remanence are markedly changed. The presence and extent of low-temperature oxidation can be recognized by reflection microscopy and by the thermomagnetic analysis and X-ray diffraction analysis.

Secular Variation

Unlike sediments, igneous rocks provide essentially spot readings of magnetic field variations in the past. It is well known that geomagnetic field changes of few tens of degrees in direction occur in less than a thousand years. Therefore, to obtain a field direction representing the axial dipole, it is essential to average out such effects of secular variation. The period necessary to do so is currently estimated to be about 10^4 to 10^6 years (McElhinny and Merrill, 1975). If the samples are not distributed over this period, we may obtain mean field directions which are different from the axial dipole field direction by 10 to 20°, depending on different models.

Wilson (1970, 1971) suggested that the geomagnetic dipole has been permanently offset from the center of the earth by a few hundred kilometers. The effect of this dipole offset on magnetic inclination is less than 2 or 3°, which is significant but which may be neglected in our case in comparison with other uncertainties.

In summary, several samples from a cooling unit are necessary to eliminate experimental errors and local anomalies and to obtain the field direction at the time of rock formation. IRM and VRM effects may be taken care of by stepwise AF demagnetization. Reflection microscopy and X-ray diffraction and thermomagnetic analyses are needed to study the possible occurrence of low-temperature oxidation. When low-temperature oxidation is present, careful consideration of the results is necessary. To eliminate the effect of secular variation and to obtain a meaningful paleolatitude (within ±5°), we may perhaps need more than 20 cooling units covering a period of at least 10^4 years and *distributed evenly in time.*

Shipboard Equipment

Remanent magnetization was measured on a Digico Balanced Fluxgate Rock Magnetometer. The spinner magnetometer was calibrated frequently for both direction and intensity, using a shipboard standard. The direction of magnetization was reproducible to within half a degree, and the drift in intensity was typically about 0.2 per cent per hour.

A Schönstedt A.C. Geophysical Specimen Demagnetizer (Model GSD-1) and a Schönstedt Thermal Specimen Demagnetizer (Model TSD-1) were available for AF and thermal demagnetization of rock samples. Because the AF demagnetizer is a single-axis system without sample tumbler, each demagnetization step required that the sample be demagnetized along each of its three orthogonal axes.

A Bison Magnetic Susceptibility System (Model 3101) was used for measuring initial susceptibility of samples.

Procedures

Minicores of 2.54 cm diameter were cut from the halved sections of the main core where orientation marks had been carefully scribed on the surface. The minicores were then sawed to approximately 2.3 cm lengths.

Normal procedure was to measure directions and intensities of the NRM and remanences in the samples after stepwise AF demagnetization of 25, 50, 100, 200, 300, 400, and 500 Oe. Some samples were demagnetized to 1000 Oe. After the measurement of remanences, initial susceptibility was measured for the same sample. Because the susceptibility meter was calibrated for samples with 2.54 cm diameter and length greater than 5 cm, a correction for a shorter length was necessary. The correction factor for variable lengths of minicores was determined from measurements of Oshima 1951 basalt samples with different lengths.

Results and Discussion (Hole 430A)

Table 8 presents a summary of paleomagnetic data obtained from 22 samples from Hole 430A. The inclination of stable remanence was determined by inspecting the intensity decay diagram and the direction change plotted on an equal-area net. The median demagnetizing field (MDF) is the value of peak alternating field required to reduce the intensity of remanence to half the

TABLE 8
Paleomagnetism, Hole 430A

Sample (Interval in cm)	Unit	Sub-bottom Depth (m)	J_{NRM} ($\times 10^{-5}$ emu/cm^3)	Inclination of NRM (°)	Stable Inclination (°)	(AF) (Oe)	MDF (Oe)	Suscept. χ ($\times 10^{-5}$)	Q_n (Oe)[b]
4-1, 53-55	SS	57.53	0.45	-46.7	-43.8	300	166	1.50	0.75
4-1, 107-109	SS	53.70	0.44	-43.5	-42.4	300	149	1.55	0.70
4-2, 50-52	SS	58.51	0.35	-44.3	-42.4	300	140	1.21	0.72
4-2, 79-81	SS	54.92	0.38	-50.9	-44.2	300	160	1.53	0.61
4-2, 88-90	1	58.89	11.30	-19.6	-16.2	200	282	2.70	10.25
4-2, 142-144	1	59.43	13.90	-24.4	-22.0	200	279	2.74	12.41
5-1, 5-7	1	66.55	5.18	-14.6	-13.9	200	296	1.77	7.18
5-1, 16-18	1	66.66	6.17	-24.9	-23.9	200	297	2.04	7.42
5-2, 21-23	1	68.27	3.27	-18.3	-16.9	200	290	1.85	4.32
5-2, 30-32	1	68.37	1.63	-16.7	-17.5	THD[a]		2.47	1.62[c]
5-2, 89-91	1	68.96	1.42	-42.5	-19.9	200	78	2.56	1.36
5-2, 120-122	1	69.27	1.44	-26.1	-15.9	200	74	2.49	1.42
5-3, 107-109	1	70.66	1.07	-42.6	-33.6	THD		2.96	0.88[c]
5-3, 140-142	1	70.98	2.77	-17.0	-15.9	200	107	2.57	2.64
5-4, 132-134	2	72.46	16.80	-11.4	-11.4	300	300	2.44	16.85
5-5, 44-46	2	73.15	7.18	-19.8	-20.2	THD[a]		1.78	9.87
5-5, 76-78	2	73.46	5.08	-19.0	-17.8	300	312	1.59	7.83
5-5, 103-105	2	73.75	4.88	-16.6	-20.9	THD		1.85	6.48
5-5, 126-128	2	73.97	6.27	-22.7	-21.6	300	322	1.78	8.63
6-1, 33-35	2	76.31	3.95	-27.7	-24.0	300	286	1.80	5.39
6-1, 67-69	2	76.60	5.58	-10.0	-10.1	THD[a]		1.88	7.26
6-1, 88-90	2	76.79	5.41	-13.0	-12.4	THD[a]		1.77	7.48
6-2, 54-56	3	77.61	3.56	-23.7	-25.0	THD[a]		1.55	5.64
6-2, 74-76	3	77.76	5.11	-25.9	-24.2	300	292	1.73	7.25
6-2, 102-104	3	78.02	4.54	-25.1	-22.4	300	324	1.61	6.90
6-2, 122-124	3	78.19	4.13	-20.8	-20.5	THD[a]		1.83	5.54
6-3, 55-57	3	78.86	3.92	-20.4	-18.3	300	322	1.83	5.24
6-3, 68-70	3	78.97	5.54	-25.0	-24.1	300	356	1.72	7.90
6-4, 8-10	4	79.79	6.36	-20.4	-18.9	300	334	1.74	8.97
6-4, 15-17	4	79.87	5.40	-18.4	-18.6	THD[a]		2.01	6.59
6-4, 143-145	5	80.78	2.90	53.2	59.0	300	116	2.57	2.77

[a]THD = Thermal demagnetization.
[b]Königsberger ratio Q_n calculated using geomagnetic intensities given in Kono (this volume).
[c]Not used in the calculation of the flow mean inclination.

NRM intensity, and is a good measure of stability of the NRM. The Q_n' ratio is defined as

$$Q_n' = J_{NRM}/\chi$$

where J_{NRM} is the intensity of the NRM and χ the initial susceptibility. Q_n' is related to the Königsberger ratio, Q_n, defined by

$$Q_n = J_{NRM}/(\chi \cdot H),$$

where H is the intensity of the earth's field. Q_n shows the relative importance of remanent magnetization in the total (remanent and induced) magnetic moment.

Typically, about two thirds of the original NRM in sandstones is lost by AF demagnetization at 200 Oe. The direction of magnetization changes irregularly by about 5° in AF steps to about 300 Oe, but at higher fields the direction changes more erratically. Since it is evident that these samples contain considerable soft components of magnetization (see the Q_n ratios in Table 8), the erratic behavior at higher demagnetizing fields may be attributed to the creation of a spurious component in the demagnetizing process.

Two types of behavior were observed in the demagnetization of basalt samples. The first is similar to that for the sandstone samples; most of the remanence is lost at a low demagnetizing field, and the direction of magnetization changes irregularly, although the range of directional change is usually smaller than that for sandstones. The second type of sample has high DMF (about 300 Oe), and shows virtually no change in the direction of magnetization during the whole demagnetizing process. We can conclude that samples of both types of basalts (and also sandstones) exhibit directions of primary components, since there is no systematic difference between inclinations of two different types belonging to the same cooling unit, and since they are quite different from the direction of the nearest geomagnetic field.

The change is inclination, MDF, and initial susceptibility with depth from the sea floor is shown in Figure 15. A large scatter of inclinations is apparent for Flow Units 1 and 2, whereas grouping is substantially better for the sandstone and Flow Unit 3. The inclination in

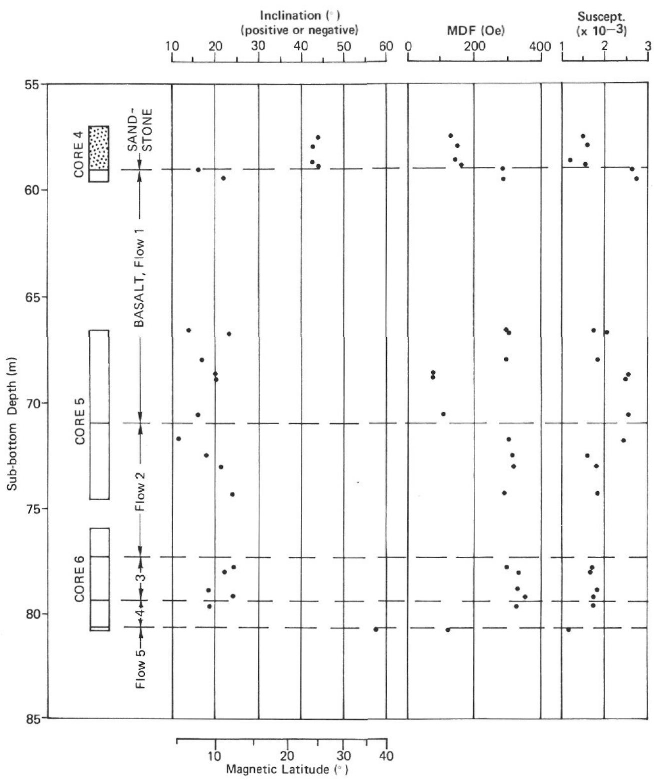

Figure 15. *Inclination, MDF, and magnetic susceptibility against sub-bottom depth in Hole 430A.*

sandstone is significantly different from inclinations in the basalt flows below; within basalt flows the inclinations are not much different, except perhaps in Flow Unit 5. Flow Unit 5 is represented by a piece of core recovered from the drill bit when the drilling operations failed after Core 6. Although the inclination can thus be measured, it is perhaps premature to conclude from a single measurement on this sample that a significant change in the magnetic field direction took place between deposition of Flow Unit 4 and of Flow Unit 5.

It is worth noting that magnetically soft samples were obtained from the lower, massive part of the Flow Unit 1. In other parts, including the topmost layers, the samples showed a magnetically stable behavior irrespective of the presence of clay in the vesicles. The lowermost massive part was not sampled in other flows. (Because Section 6-4 was recovered in the drill bit after the operation terminated, the lower part of Flow Unit 3 is probably not represented in the recovered cores).

PHYSICAL PROPERTIES

Sonic velocity and density were measured on samples recovered from Holes 430 and 430A. The P-wave velocity was measured by finding the time (about 10 μm) for a sonic pulse to travel across a sample about 3 cm thick. The samples could be aligned to measure velocities along the direction of the core or perpendicular to the core, and slight velocity anisotropy was observed. Density was measured by a gamma-ray absorption technique, using the GRAPE machine. (For a given path length between source and detector, the per cent of gamma rays absorbed depends upon the total mass in this absorbing column, relatively independently of the chemistry of the mass. Thus, by measuring the total absorption and the distance across the sample, the density of the sampling can be calculated.) The apparatus has two modes of operation, analog and fixed. In the analog mode, the core moves slowly past the source-detector on a motorized track, and the core diameter at selected points is later measured with calipers and collated with the analog record of gamma absorption versus distance along the core. In the fixed mode, the sample is stationary and a scaler counts the gamma rays for a fixed two minutes, which yields a statistically better value than the analog mode, in which 1 cm of core traverses past the detector in about 6 seconds. Details on the operation of these instruments and the methods used to calibrate them are given in an appendix.

Tables 9 and 10 and Figures 16 and 17 present the data for Site 430. In Hole 430, the velocity increased from 1.8 to 2.0 km/s from the sea floor to 4 meters downhole; this corresponds to a lithologic change from fine sand to coarser sand to sand and pebbles (a gradation that may well have occurred in the core barrel as a consequence of pumping while drilling.[3] One lithologically similar sample from Hole 430A was measured: Sample 430A-2-1, 123 cm (calcareous sand and volcanic fragments) has a very similar velocity. The material below the loose sand in Hole 430A is gray sandstone. The boundary between these units was not evident in the physical properties data, because of poor recovery. Pieces selected to be representative of the gray sandstone unit all have about the same velocity and density (3.0 km/s; 2.2 g/cm^3); these values decrease about 10 per cent near the contract with basalt below. A velocity anisotropy occurs in this unit; the vertical velocities are about 3 per cent less than the horizontal velocities. The wet bulk density and dry bulk density of this sandstone were determined in the chemistry lab by weighing a known volume of material before and after baking. The densities obtained by these different methods are in good agreement. The porosity (29%) measured by this dry bulk/wet bulk method agrees well with the porosity (26%) of a neighboring sample obtained from loss-on-ignition during prepartion of an XRF sample.

Below the sandstone are four flows of compositionally similar basalt (hawaiite). All the flow units identified by the petrologists have distinct physical properties (Table 9). The topmost basalt measured (Sample 430A-4-2, 145 cm) has a lower than typical velocity and densi-

[3] Note: the recovery in Core 2 (7.9 m) is more than the interval drilled (from 2.5 m sub-bottom to 4.5 m). We assume that the larger O.D. drill pipe extruded its displaced volume of soft material into the small I.D. of the core barrel. The sub-bottom depths given here and in Tables 9 and 10 are calculated by the formula depth equals sub-bottom depth to the top of the cored interval plus 1.5 meters times the number of sections above, plus the centimeter location of the sample as it is now in the section. This is one of four possible configurations of core in the core barrel where the formula leads to contradictory results; sub-bottom depths not calculated by this rule are marked with a dagger †.

TABLE 9
Velocity Measurements, Site 430

Core-Section, Sample Location (cm)	Sub-bottom Depth (m)	Velocity, Horizontal (km/s)	Velocity, Vertical (km/s)
Hole 430			
2-3, 3	1.02†	1.83 ± 0.03	
2-4, 7	3.05†	1.92 ± 0.04	
2-4, 116	3.78†	2.00 ± 0.05	
Hole 430A			
2-1, 123	20.23	1.68 ± 0.03	
4-1, 45	57.45	3.13 ± 0.05	3.06 ± 0.01
4-1, 107	58.07	2.95 ± 0.03	2.86 ± 0.01
4-2, 79	59.29	2.89 ± 0.03	2.68 ± 0.01
4-2, 142	59.92	4.51 ± 0.01	4.40 ± 0.02
5-2, 140	69.40	5.16 ± 0.04	
6-4, 12	80.62	5.06 ± 0.01	
6-4, 146	81.96	5.82 ± 0.03	

Note: Errors listed are for the reproducibility within the sample, not how the sample represents the core or the sea floor. The first four measurements were made through the core liner. See Introduction and Footnote 3, this chapter, for explanation of the sub-bottom depths marked †.

ty. This sample contains only 1 or 2 per cent clinopyroxene, as is typical at the top of a flow; low abundances of clinopyroxene produce lower velocity and density. The vertical velocity of this sample is less than its horizontal velocity; this anisotropy may be caused by feldspars aligned horizontally. Detailed sampling began about 50 cm below the next identified flow boundary. The initial increase in density with depth here probably reflects increasing amounts of clinopyroxene away from the top of the flow, inasmuch as there are no vesicles at this flow boundary. The boundaries at 71 and 77 meters sub-bottom are marked by dramatic drops in density; these reflect areas of many large vesicles.

As fate would have it, the last piece recovered — the piece that was jammed sideways in the bit — is chemically distinct and appears to be a part of another unit. This sample, which is a porphyritic basalt with phenocrysts of plagioclase and clinopyroxene, has a velocity and density notably higher than the stratigraphically higher samples.

CORRELATION OF SEISMIC PROFILES WITH DRILLED SEQUENCE

Ōjin Seamount is acoustically complex, as are most of the Emperor Seamounts. Almost everywhere, acoustic basement lies close to the surface. Irregular relief, the hard surface, and this thin sediment cover prevent good definition of structures. Nevertheless, fairly well defined sedimentary units can be locally distinguished in the seismic profiles. The acoustic stratigraphy in the vicinity of Site 430 is shown in the seismic reflection profiles obtained aboard the *Glomar Challenger* (Figure 4), and represents sediment filling an acoustic basement basin (Figure 18). No distinct sedimentary units can be identified in this basin, because the entire sedimentary

TABLE 10
Density Measurements, Site 430

Hole-Core-Section, Sample Location (cm)	Sub-bottom Depth (m)	GRAPE Density, Unless Noted Otherwise (g/cm^3)	Porosity (%)
430-2-4, 10	3.07[a]	1.85	
430-2-4, 20	3.14[a]	1.85	
430-2-4, 30	3.20[a]	1.87	
430-2-4, 40	3.27[a]	1.88	
430-2-4, 50	3.34[a]	1.86	
430-2-4, 60	3.40[a]	1.87	
430-2-4, 70	3.47[a]	1.88	
430-2-4, 80	3.54[a]	1.91	
430-2-4, 90	3.60[a]	1.93	
430-2-4, 100	3.67[a]	1.93	
430-2-4, 110	3.74[a]	1.93	
430-2-4, 120	3.80[a]	1.91	
430-2-4, 130	3.87[a]	1.89	
430-2-4, 140	3.94[a]	1.84	
430A-4-1, 45	57.45	2.18[b]	
430A-4-1, 45	57.45	2.32[c]	29
430A-4-1, 69	57.69	d	26
430A-4-1, 95	57.95	2.29	
430A-4-1, 100	58.00	2.26	
430A-4-1, 105	58.05	2.27	
430A-4-1, 107	58.07	2.21[b]	
430A-4-2, 41	58.91	2.24	
430A-4-2, 45	58.95	2.24	
430A-4-2, 48	58.98	2.24	
430A-4-2, 79	59.29	2.15[b]	
430A-4-2, 145	59.92	2.66[b]	
430A-5-1, 6	66.56	2.64	
430A-5-1, 19	66.69	2.68	
430A-5-1, 31	66.81	2.63	
430A-5-1, 38	66.88	2.56	
430A-5-1, 52	67.02	2.66	
430A-5-1, 60	67.10	2.70	
430A-5-1, 75	67.25	2.66	
430A-5-1, 82	67.32	2.64	
430A-5-1, 88	67.38	2.70	
430A-5-1, 96	67.46	2.75	
430A-5-1, 105	67.55	2.67	
430A-5-1, 115	67.65	2.68	
430A-5-1, 125	67.75	2.72	
430A-5-1, 135	67.85	2.67	
430A-5-1, 144	67.94	2.64	
430A-5-2, 4	68.04	2.66	
430A-5-2, 24	68.24	2.71	
430A-5-2, 35	68.35	2.68	
430A-5-2, 45	68.45	2.72	
430A-5-2, 64	68.64	2.73	
430A-5-2, 84	68.84	2.73	
430A-5-2, 109	69.09	2.75	
430A-5-2, 123	69.23	2.75	
430A-5-2, 133	69.33	2.75	
430A-5-2, 143	69.43	2.77	
430A-5-2, 145	69.45	2.77[b]	
430A-5-3, 10	69.60	2.71	
430A-5-3, 25	69.75	2.72	
430A-5-3, 40	69.90	2.75	
430A-5-3, 58	70.08	2.75	
430A-5-3, 85	70.35	2.74	
430A-5-3, 94	70.44	2.72	
430A-5-3, 108	70.58	2.74	
430A-5-3, 125	70.75	2.75	
430A-5-3, 140	70.90	2.76	

TABLE 10 – *Continued*

Hole-Core-Section, Sample Location (cm)	Sub-bottom Depth (m)	GRAPE Density, Unless Noted Otherwise (g/cm^3)	Porosity (%)
430A-5-4, 5	71.05	2.73	
430A-5-4, 12	71.12	2.67	
430A-5-4, 20	71.20	2.68	
430A-5-4, 29	71.29	2.57	
430A-5-4, 104	72.04	2.45	
430A-5-4, 112	72.12	2.36	
430A-5-5, 13	72.63	2.45	
430A-5-5, 49	72.99	2.39	
430A-5-5, 56	73.06	2.36	
430A-5-5, 79	73.29	2.54	
430A-5-5, 88	73.39	2.63	
430A-5-5, 109	73.58	2.69	
430A-5-5, 127	73.77	2.71	
430A-5-6, 6	74.06	2.70	
430A-6-1, 6	76.06	2.70	
430A-6-1, 19	76.19	2.67	
430A-6-1, 32	76.32	2.74	
430A-6-1, 58	76.58	2.69	
430A-6-1, 67	76.67	2.73	
430A-6-1, 86	76.86	2.70	
430A-6-1, 99	76.99	2.66	
430A-6-1, 140	77.40	2.29	
430A-6-2, 6	77.56	2.41	
430A-6-2, 17	77.67	2.38	
430A-6-2, 28	77.78	2.28	
430A-6-2, 53	78.03	2.37	
430A-6-2, 77	78.27	2.60	
430A-6-2, 88	78.38	2.64	
430A-6-2, 103	78.53	2.68	
430A-6-2, 116	78.66	2.66	
430A-6-2, 135	78.85	2.72	
430A-6-3, 5	79.05	2.72	
430A-6-3, 27	79.27	2.70	
430A-6-3, 58	79.58	2.73	
430A-6-3, 70	79.70	2.68	
430A-6-4, 10	80.60	2.73[b]	
430A-6-4, 14	80.64	2.75[b]	
430A-6-4, 145	81.95	2.91[b]	

[a]See Introduction and Footnote 3, this chapter, for explanation of these sub-bottom depths.
[b]Two-minute GRAPE count.
[c]Wet bulk density (known volume weighed).
[d]Porosity from loss on ignition.

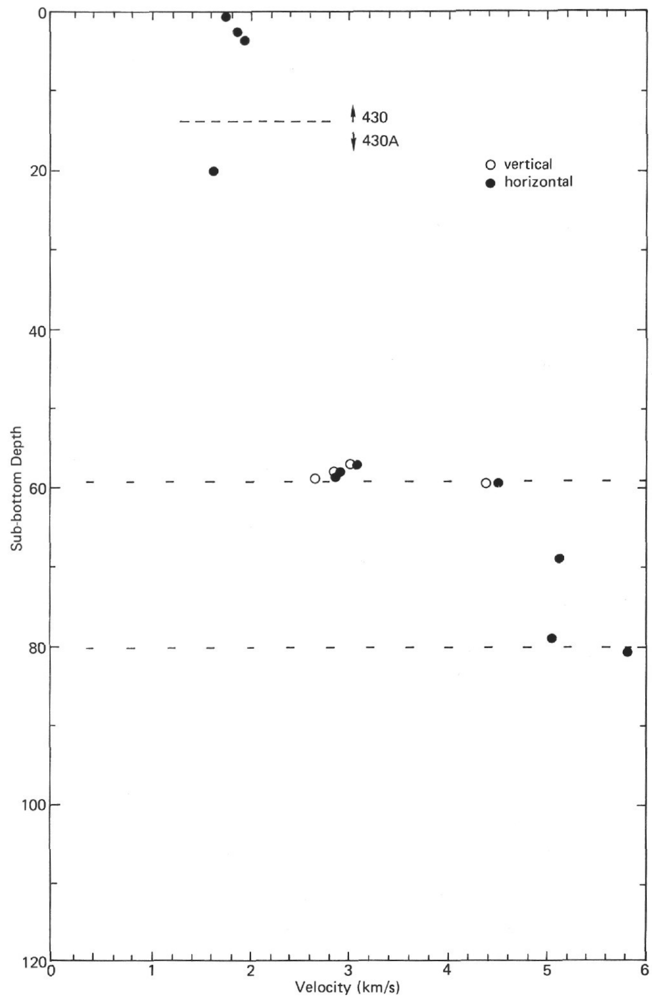

Figure 16. *Sonic velocity versus sub-bottom depth for Site 430.*

sequence is composed of alternating strong and weak, rather uniformly spaced reflectors, most of which are short and discontinuous. Several strong reflectors are continuous throughout the basin, and are approximately 0.1, 0.15, and 0.18 s beneath mudline. All reflectors appear flat-lying, with small, local undulations and slight upturns against the acoustic basement at the margins of the basin.

The surface of the acoustic basement does not appear as a strong reflector on any profile crossing the sedimentary basin. Instead, acoustic basement is an ill-defined zone, underlain by random reflectors or noise; the surface is locally irregular and U-shaped in profile. Depth to acoustic basement varies from about 0.02 s near the margin of the basin to nearly 0.18 s in the central part.

Site 430 is at the northeast margin of the basin. In this region only a few continuous reflectors overlie the acoustic basement identified at a sub-bottom depth of approximately 0.06 s. Unfortunately, the bubble pulse on the profiles collected on board the *Glomar Challenger* is about 0.1 s long (velocity of 1.5 km/s assumed); this masks about the upper 75 meters of subsurface stratigraphy.

The broad bubble pulse allows us to correlate only the lower half of the core recovered at Hole 430A with the seismic profiles (Figure 19). The first strong reflector (0.1 s) is deeper than the total depth of Hole 430A. The calcarenite and ash layers recovered in the core appear as weak, discontinuous reflectors immediately beneath the bubble pulse (Figure 19). A weak reflector, immediately above a zone of random reflectors identified in the seismic reflection profile at 0.06 s beneath the mudline, is apparently the basement surface. The velocity of 1.68 km/s derived from calcareous sands in the core from Hole 430A (see Physical Properties, this site) gives a calculated depth to acoustic basement of 50.4 meters. We first cored basalt at 59.3 meters below mudline in Hole 430A.

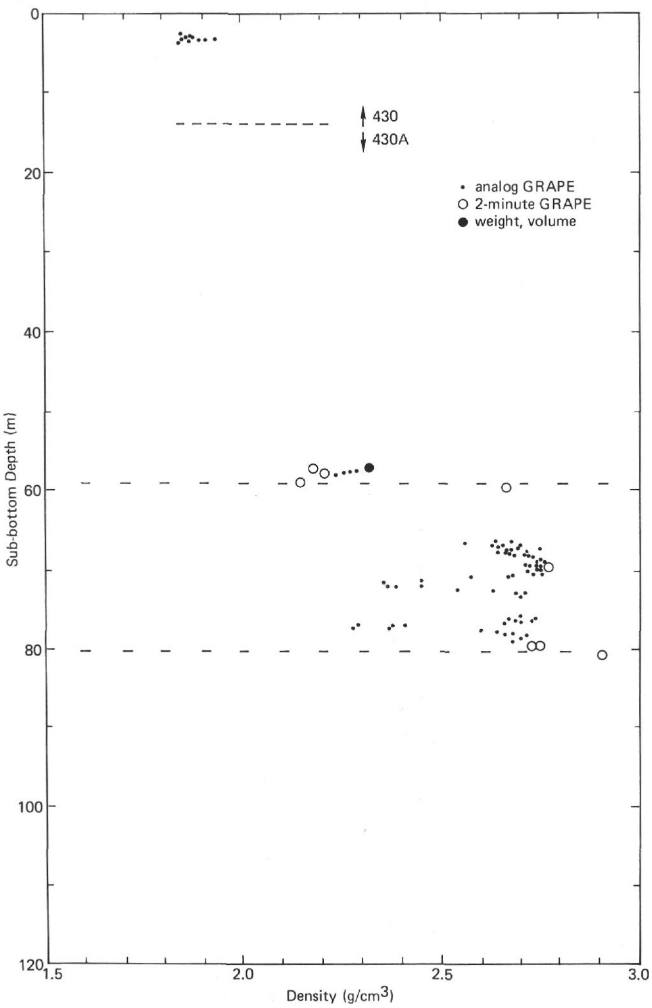

Figure 17. *Density versus sub-bottom depth for Site 430.*

The 3.5-kHz profile obtained aboard the *Glomar Challenger* (Figure 10) does not show well-layered internal reflectors. Directly over the site, the 3.5-kHz profile shows an undulating upper surface beneath which irregular and somewhat transparent acoustic characteristics are prominent. This reflection characteristic represents the unconsolidated, water-saturated silt, clay, and pebbly mud recovered in the upper parts of cores from Holes 430 and 430A.

We attempted no sonobuoy profiles at this site, because the stratigraphic units drilled are restricted to a small (approximately 6 km diameter) basin, and the surrounding bottom topography is irregular. We initially assumed that average seismic velocities were 2.5 km/s, but adjusted this value to 1.68 km/s on the basis of physical property measurements on sediments cored in Hole 430A.

SUMMARY AND CONCLUSIONS

Despite the difficulties of drilling at this site and the forced termination of Hole 430A after penetrating only 118 meters, the principal objectives were met.

Both the petrography and chemistry of the four basalt flows cored in Hole 430A demonstrate that Ōjin Seamount is of the Hawaiian type. Chemically and petrographically, Flow Units 1 through 4 in Hole 430A are hawaiites very close in composition to the average hawaiite (MacDonald, 1968), if somewhat richer in P_2O_5. Although Flow Unit 5 is slightly lower in SiO_2 and MgO contents and higher in Al_2O_3 and CaO contents than the average Hawaiian tholeiite, it is nonetheless a tholeiite within the compositional range of known Hawaiian tholeiites. It may have been erupted during the caldera-filling or post-caldera stage, or it may have come from a shield-building flow. The discovery of both tholeiitic basalt and hawaiite in Hole 430A shows that Ōjin volcano is of the Hawaiian type, as predicted by the hot-spot hypothesis, and probably was constructed by a sequence of eruptive stages typical of Hawaiian volcanoes, although a post-erosional stage can neither be confirmed nor denied.

Both the volcanic and sedimentary rocks recovered at Site 430 show that Ōjin (and its shallower and adjoining neighbor, Jingū) once stood as islands above the sea. Flow Units 1 through 4 are massive with coarse vesicular tops, partly oxidized in places, and resemble subaerial Hawaiian flows. There is a complete absence of pillow structures or any other features that would even suggest underwater eruption. In addition, part of a red, oxidized soil zone, which could only have formed subaerially, was recovered between Flow Units 3 and 4. The sediments and fossils recovered in Hole 430 and above the basalt in Hole 430A are typical of shallow-water reef and littoral environments. In particular, the presence of coarse-grained volcanogenic sands and calcarenites, well-rounded volcanic pebbles, fragments of corraline algae, benthic foraminifers, oolites, ostracodes, and fragments of echinoderms, gastropods, and bivalves, all indicate deposition within 10 meters of sea level.

On the basis of seismic evidence, Greene et al. (1978) have proposed that the principal volcanoes of the Emperor Seamount chain, at least as far north as Suiko Seamount, are all capped by coral reefs, which ceased to grow no later than the late Eocene because of the rapid drop in ocean surface temperature at the time. By the time the surface temperature warmed sufficiently to permit coral growth in the middle or late Miocene, movement of the Pacific plate had carried the seamounts too far north to permit reef development. The fossils recovered from Site 430 substantiate this argument. Calcareous nannofossils found in Core 2, Hole 430, are assigned to Zones NP 19 to NP 20 (Martini, 1971) and indicate a late Eocene date. In Hole 430A, the sediments above the basalt in Core 3 contain abundant calcareous nannofossils assigned to NP 9 Zone (upper Paleocene), and upper Paleocene to lower Eocene planktonic foraminifers. The punch core at Hole 430B yielded Quaternary calcareous and siliceous microfossils. Thus, at Site 430 the youngest indications of shallow-water reef environment are middle Eocene.

The upper Paleocene calcareous nannofossils in the sediments above the basalt suggest that Ōjin Seamount may be older than Kōkō Seamount, on which lower Eocene fossils were found (Larson, Moberly, et al., 1975). Although the species diversity in the Site 430 fossil

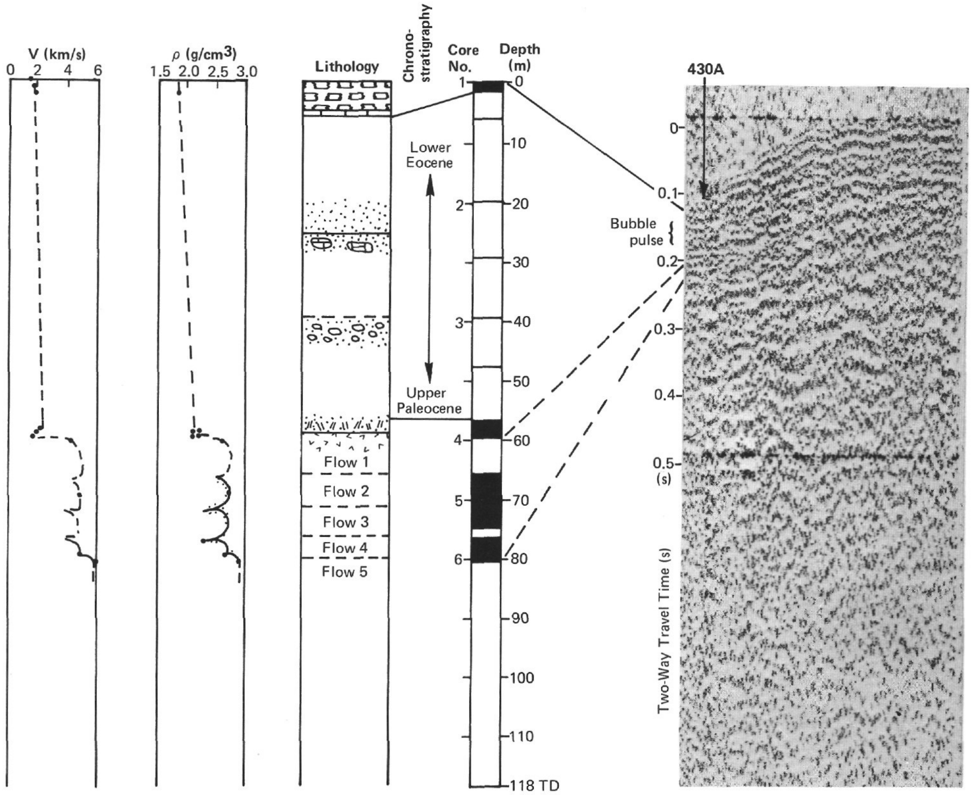

Figure 18. *Correlation of seismic reflection profile with physical properties and lithologic column, Hole 430A.*

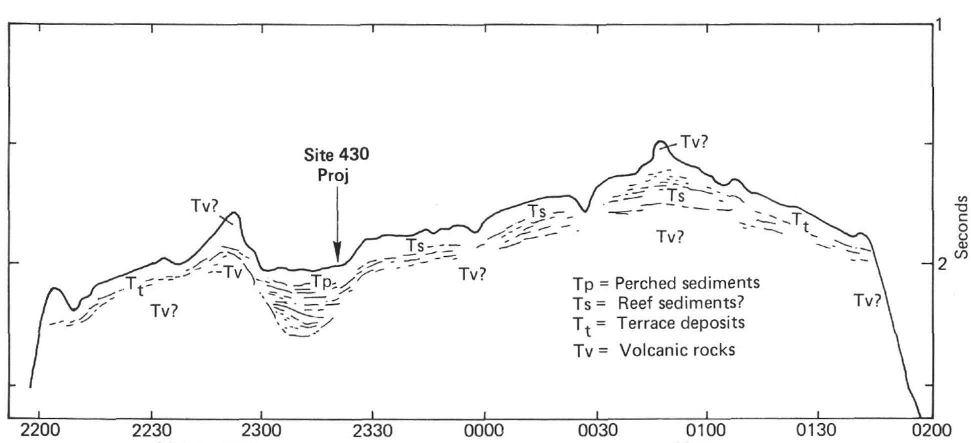

Figure 19. *Line drawing of seismic reflection profile obtained by the* S.P. Lee *across Ōjin Seamount, showing geologic interpretation of acoustic units, Site 430.*

material was low, this tentative shipboard conclusion as to the relative ages of Kōkō and Ōjin seamounts has been substantiated by subsequent K-Ar dating of the basalt flows (Dalrymple et al., this volume).

REFERENCES

Bougault, M., Cambon, P., and Toulhoat, H., 1977. X-ray spectometric analysis of trace elements in rocks, *X-ray Spectrometry*, v. 6, p. 66–72.

Chase, T. E., Menard, H. W., and Mammerickx, J., 1970. *Bathymetry of the North pacific, Charts 2, 7, 8:* Inst. Marine Resources, Scripps Institution of Oceanography.

Clague, D. A., 1974. The Hawaiian-Emperor Seamount chain: Its origin petrology and implications for plate tectonics, Ph.D. thesis, University of California, San Diego.

Clague, D. A., Dalrymple, G. B., and Moberly, R., 1975. Petrography and K-Ar ages of dredged volcanic rocks from western Hawaiian Ridge and southern Emperor Seamount chain, *Geol. Soc. Am. Bull.*, v. 86, p. 991–998.

Dalrymple, G. B., Lanphere, M. A., and Jackson, E. D., 1974. Contributions to the petrography and geochronology of volcanic rocks from the leeward Hawaiian Islands, *Geol. Soc. Am. Bull.*, v. 85, p. 727-738.

Greene, H. G., Dalrymple, G. B., and Clague, D. A., 1978. Evidence for northward movement of the Emperor Seamount, *Geology,* v. 6, p. 70–74.

Heezen, B. C., MacGregor, I. D., et al., 1973. *Initial Reports of the Deep Sea Drilling Project*, v. 20: Washington (U.S. Government Printing Office).

Larson, R. L., Moberly R. et al., 1975. *Initial Reports of the Deep Sea Drilling Project,* v. 32: Washington (U.S. Government Printing Office).

Macdonald, G. A., 1968. Composition and origin of Hawaiian lavas, *Geol. Soc. Am. Mem. 116,* p. 477–522.

________, 1969. Petrology of the basalt cores from Midway Atoll, *Geol. Survey Prof. Paper 680-B*, p. B1–B10.

Martini, E., 1971. Standard Tertiary and Quaternary calcareous nannoplankton zonation, Second Plank. Conf., Roma, Proc., 1970, p. 739–785.

McElhinny, M. W. and Merrill, R. T., 1975. Geomagnetic secular variation over the past 5 m.y., *Rev. Geophys. Space Phys.*, v. 13, p. 687–708.

Stearns, H. T., 1946a. Geology of the Hawaiian Islands, *Hawaii Div. Hydrography Bull.*, v. 8, p. 1–106.

________, 1946b. *Geology of the State of Hawaii*: Palo Alto (Pacific Books.)

Wilson, R. L., 1970. Permanent aspects of the earth's non-dipole magnetic field over upper Tertiary times, *Geophys. J. Roy. Astron. Soc.*, v. 19, p. 417–437.

________, 1971. Dipole offset — the time average paleomagnetic field over the past 25 million years, *Geophys. J. Roy. Astron. Soc.*, v. 22, p. 491–504.

SITE 430 HOLE CORE 2 CORED INTERVAL: 2.5-4.5 m

TIME–ROCK UNIT	BIOSTRAT ZONE	FORAMS	NANNOS	RADS	SILICOS	DIATOMS	SECTION	METERS	GRAPHIC LITHOLOGY	DRILLING DISTURBANCE	SEDIMENTARY STRUCTURES	LITHOLOGIC SAMPLE		LITHOLOGIC DESCRIPTION
							1	0.5, 1.0				*	10YR 3/2	
							2					G.S		
							3					*	10YR 3/3	
							4						10YR 3/3	
							5					*		
									VOID					
UPPER EOCENE	NP19 NP20	RM	RM	B	B	B	CC							

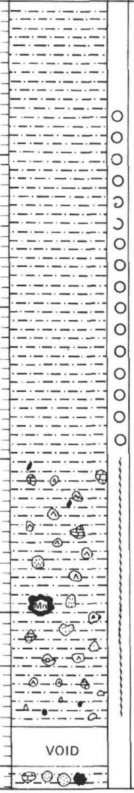

Watery muddy sand, very dark grayish brown

S.S. (at 0.80 m):
40% clastic carbonates
15% clay
15% volcanic fragments
15% Mn-micronodules
10% calcareous nannofossils
5% foraminifera
TR quartz, sponge spicules, apatite
Texture (S.S.): 55% clay, 30% silt, 15% sand

Watery muddy sand with very coarse fragments, dark brown

S.S. (at 3.60 m):
40% clastic carbonates
15% clay
15% volcanic glass
15% Mn-micronodules
5% calcareous nannofossils
5% foraminifera
5% quartz
Texture (S.S.): 55% clay, 30% silt, 15% sand

Pebbly mud - "shore line" deposits
Unconsolidated, angular and rounded clastic gravel, dark brown
Clasts: (size: 1-3 cm) rounded black → Mn-nodules (at 5.90 m)
Fragments of iron-manganese concretions
Wathered basalt, volcanic glass, cemented Mn-calcite
Limestone-fragments
Red siltstone and red chert
Brown and red mudstone

At 6.90 m color (decrease in the amount material) changes, gives appearance of black

S.S. (at 6.95 m):
50% clastic carbonates
15% clay
15% calcareous nannofossils
10% Mn-micronodules
5% volcanic fragments
5% foraminifera
TR quartz, sponge spicules
Texture (S.S.): 65% clay, 30% silt, 5% sand

CC: Pebbly mud, rounded and angular clastic gravel fragments: mudstone, siltstone, Mn-nodules, limestones
Size: 0.5 to 2 cm

Site 430, Core 1, Cored Interval: 0.0-2.5 m: NO RECOVERY

Information on core description sheets, for ALL sites, represents field notes taken aboard ship under time pressure. Some of this information has been refined in accord with post-cruise findings, but production schedules prohibit definitive correlation of these sheets with subsequent findings. Thus the reader should be alerted to the occasional ambiguity or discrepancy.

SITE 430 HOLE A CORE 1 CORED INTERVAL: 0.0-5.5 m

TIME-ROCK UNIT	BIOSTRAT ZONE	FORAMS	NANNOS	RADS	SILICOS	DIATOMS	SECTION	METERS	GRAPHIC LITHOLOGY	DRILLING DISTURBANCE	SEDIMENTARY STRUCTURES	LITHOLOGIC SAMPLE
UPPER PALEOCENE							1	0.5, 1.0	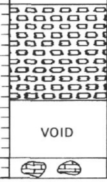			*, G.S, CC
		RM	RM	B	B	B	CC					TS

LITHOLOGIC DESCRIPTION

10YR 8/4

Silty calcareous ooze, very pale brown

Contains large altered basalt pebble at 0.3-0.53, 0.7 and 0.8 m (size ø ≃3 cm)

Contains also white chalky concretions at 0.76 and 0.94 m

S.S. (at 0.36 m):
75% clastic carbonate
25% clay
Texture (S.S.): 85% clay, 15% silt

S.S. (at 0.98 m) in white concretion:
95% clastic carbonate
5% clay
Texture (S.S.): 95% clay, 5% silt

$CaCO_3$ % interval 89-90 cm = 86%

CORE CATCHER: LIMESTONE
Two pieces nodular with vesicular, wavy structures appears to be cemented calcareous mud containing the solidified white concretions.

SITE 430 HOLE A CORE 2 CORED INTERVAL: 19.0-28.5 m

TIME-ROCK UNIT	BIOSTRAT ZONE	FORAMS	NANNOS	RADS	SILICOS	DIATOMS	SECTION	METERS	GRAPHIC LITHOLOGY	DRILLING DISTURBANCE	SEDIMENTARY STRUCTURES	LITHOLOGIC SAMPLE
UPPER PALEOCENE							1	0.5, 1.0	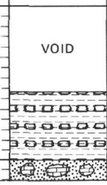			*, CC, G.S
		RP	RP	B	B	B	CC					2 TS

LITHOLOGIC DESCRIPTION

Calcareous sand with black volcanic fragments, very pale brown

S.S. (at 0.9 m) in fine material, calcareous silty mud
85% clastic carbonate
10% calcareous nannofossils
5% clay
Texture(S.S.): 90% clay, 10% silt

10YR 7/3

CC: LIMESTONE NODULES AND CALCAREOUS SAND
"Nodules" are cemented – occurence of algal concretions and volcanic materials.

SITE 430 HOLE A CORE 3 CORED INTERVAL: 38.0-47.5 m

TIME-ROCK UNIT	BIOSTRAT ZONE	FORAMS	NANNOS	RADS	SILICOS	DIATOMS	SECTION	METERS	GRAPHIC LITHOLOGY	DRILLING DISTURBANCE	SEDIMENTARY STRUCTURES	LITHOLOGIC SAMPLE
UPPER PALEOCENE	NP9	RM	FM	B	B	B	CC		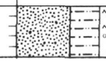			

LITHOLOGIC DESCRIPTION

Core Catcher only, eight pebbles

Calcareous sandstone, five pebbles, yellow (10YR 8/6)

S.S.:
85% unspecified clastic carbonate
10% clay
<5% calcareous nannofossils

Mudstone, two pebbles, soft brownish yellow (10YR 6/6) (ext) and dark brown (7.5YR 3/2)

S.S. exterior:
85% unspecified clastic carbonate
10% clay
5% calcareous nannofossils
TR volcanic glass and micronodules

S.S. interior:
40% unspecified clastic carbonate
35% clay
15% quartz
5% volcanic glass
5% micronodules

Altered vesicular basalt, one pebble, dark brown (10YR 3/2)

SITE 430 HOLE A CORE 4 CORED INTERVAL: 57.0-66.5 m

TIME-ROCK UNIT	BIOSTRAT ZONE	FORAMS	NANNOS	RADS	SILICOS	DIATOMS	SECTION	METERS	GRAPHIC LITHOLOGY	DRILLING DISTURBANCE	SEDIMENTARY STRUCTURES	LITHOLOGIC SAMPLE
							1	0.5, 1.0	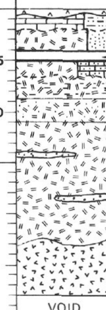			TS, CC, CC
							2					TS
		VRP	B	B	B	B	CC					

LITHOLOGIC DESCRIPTION

VOID

Altered basalt 7.5YR 4/3 (pebble), calcareous sandstone, sandy mud; "calcarenites" tuff and calcareous sandstone (7.5YR 3/0 and 7.5YR 7/4) mud and ash layer

"silty-sandy" ash (2.5Y 3/0)

Sandstone layers "calcarenites" interbanded with dark gray ash layers

Dark gray basalt (crystalline flow) with interlayed fine beds of calcareous material

2.5Y 4/0

2.32-2.41 m: very dark (2.5Y 3/0), lightly altered, aphyric <1% irregular vesicles (~ 1 mm). Some vesicles are calcite filled. The groundmass is fine-grained plagioclase, pyroxene and olivine (mostly fresh). There are 6 fractures ⊥ to core length filled with calcite.

2.41-2.60 m: *less altered than above, fewer fractures and* filled calcite vesicles

2.60-2.69 m: basalt, same as above, quite fresh

S.S. (at 0.30 m), only soft part of sediment, volcanic sand:
60% volcanic glass
15% clay
15% clastic carbonate
5% quartz
5% feldspar
TR heavy minerals
Texture (S.S.): 60% sand, 20% silt, 20% clay

$CaCO_3$ % interval 71-92 cm = 0%

VISUAL CORE DESCRIPTION FOR IGNEOUS ROCKS

LEG **55** SITE **430** HOLE **A** CORE **5** DEPTH **66.5-76.0 m**

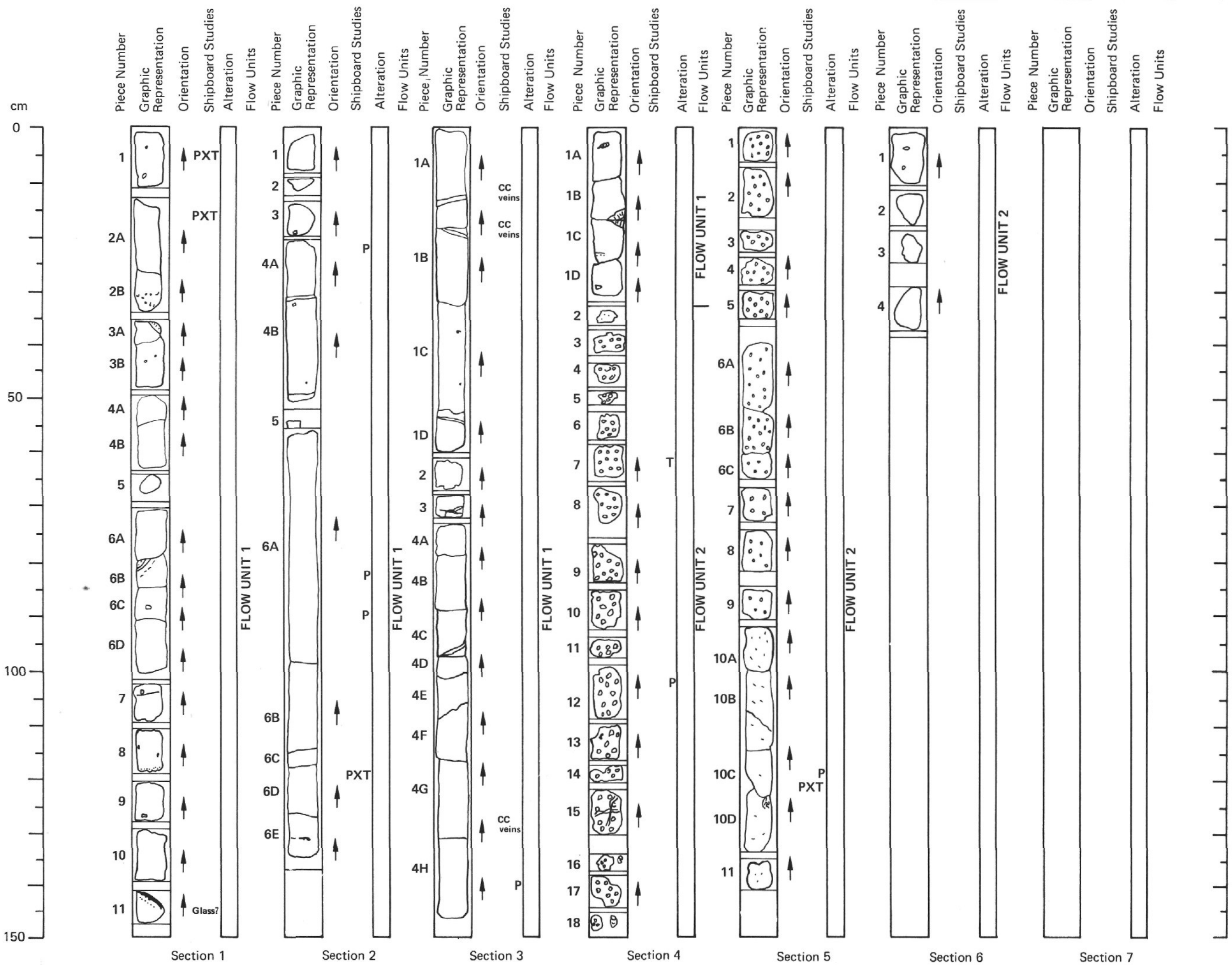

FLOW UNIT NO. 1:

POSITION: Top - Core 4, Sect. 2, 80 cm; Bottom - Core 5, Sect. 4, 32 cm
CHEMISTRY: Hawaiite, 4 analyses in Table 1.

VISUAL DESCRIPTION

Mineralogy: Phenocrysts: essentially aphyric, a very few altered olivines and fresh pyroxenes
Groundmass: plagioclase (sub-trachytic), pyroxene, and rare olivine
Lithology: Dense, essentially non-vesicular (a few calcite filled vesicles), flow top ended, flow bottom slightly more vesicular
Alteration: Mostly fresh

THIN SECTION DESCRIPTION

Phenocrysts: Ol. <1%, 0.5-3 mm, subhedral, iddingsitized: plag. <1%, 0.5-2 mm, tabular to subhedral, some embayed
Groundmass: Ol. 1% in top of flow, 0.05 to 0.2 mm, anhedral to subhedral, iddingsitized; plag. 45-60%, 0.05-0.5 mm laths ($An_{30\pm}$); cpx. 10-15%, 0.01-0.2 mm, sub-ophitic to anhedral; opaque 5-15%, up to 0.2 mm, euhedral to anhedral, apatite, to 1%, to 0.2 mm long, acicular
Texture: Sub-trachytic, sub-ophitic
Vesicles: <1%
Alteration: 5-20% clay replacing interstitial glass and olivine

MAGNETIC DATA

Average Inclination: −18.6° (±2.5)
Average Magnetic Intensity (10^{-5} Gauss): 560

FLOW UNIT NO. 2:

POSITION: Top - Core 5, Sect. 4, 34 cm; Bottom - Core 6, Sect. 1, 109 cm
CHEMISTRY: Hawaiite, 2 analyses in Table 1.

VISUAL DESCRIPTION

Mineralogy: Phenocrysts: 3-4% altered of microphenocrysts at very top, mostly aphyric
Groundmass: fine- to medium-grained, ol. 15%, plag. 50%, px. + op. 35%
Lithology: Flow top has 15-20%, 2-6 mm vesicules (lined by clay and some calcite filled) — top oxidized (2.5YR 3/2): progressively less vesicular downward, but a few at very bottom
Alteration: Top oxidized. Central and bottom part fresh with some unaltered groundmass olivine, other phases fresh

THIN SECTION DESCRIPTION

Phenocrysts: Plag. ≪1%, 1.8 mm, one resorbed crystal titanomagnetite - ≪1%, 0.3 mm, euhedral
Groundmass: Ol. - 0.3%, 0.01-0.4 mm, anhedral, altered to iddingsite; plag. 50-60%, 0.1-0.4 mm, laths; cpx. 5-10%, 0.1-0.2 mm, anhedral to sub-ophitic; opaque 5%, subhedral; apatite 1%, 0.1 mm
Texture: Trachytic to sub-trachytic
Vesicles: 1-25%, mostly clay lined, some calcite filled
Alteration: 10-20% clay after interstitial glass

MAGNETIC DATA

Average Inclination: − 18.7° (±5.4)
Average Magnetic Intensity (10^{-5} Gauss): 750

VISUAL CORE DESCRIPTION FOR IGNEOUS ROCKS

LEG **55** SITE **430** HOLE **A** CORE **6** DEPTH **76.0-85.5 m**

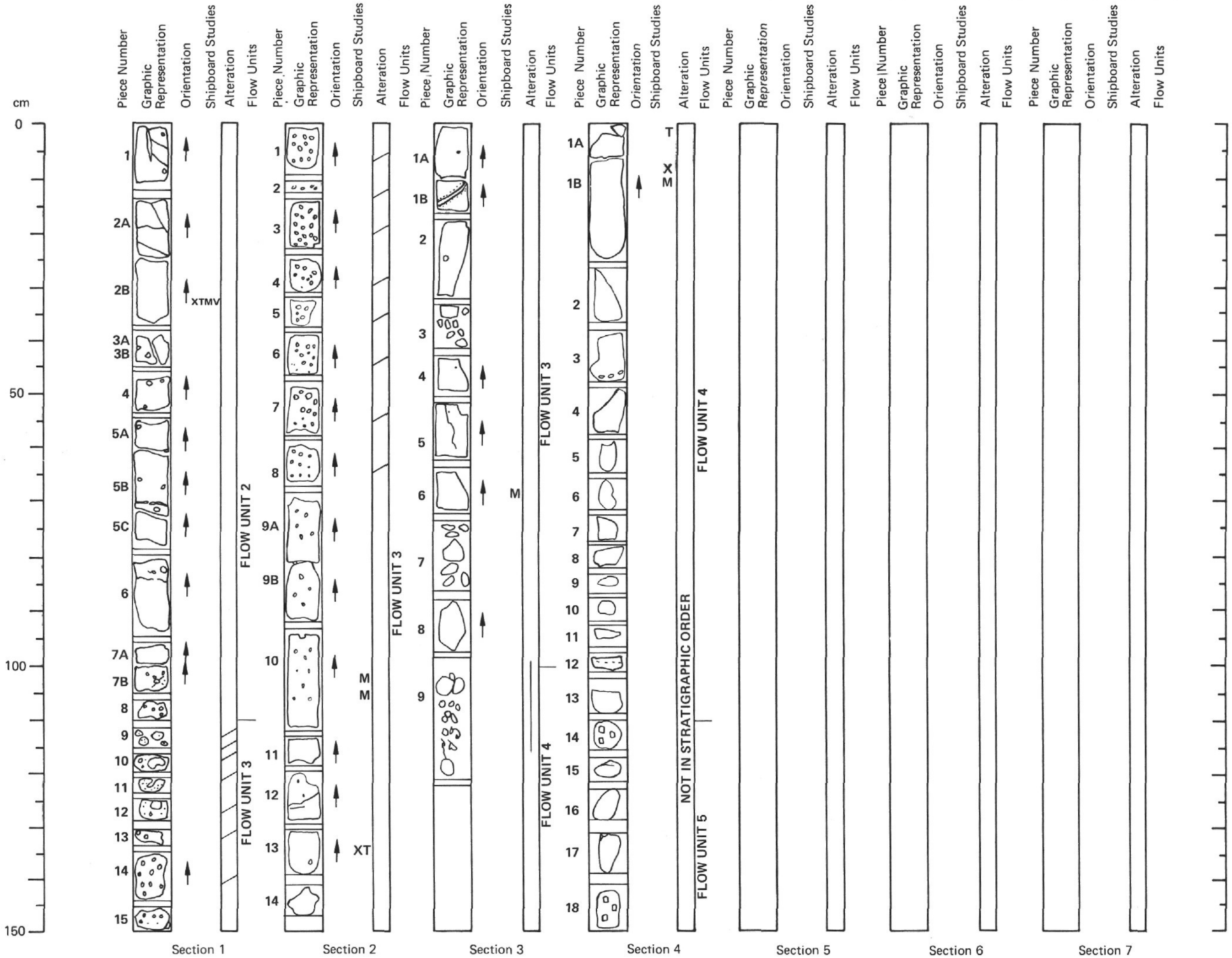

FLOW UNIT NO. 3:

POSITION: Top - Core 6, Sect. 1, 111 cm; Bottom - Core 6, Sect. 3, 99 cm

CHEMISTRY: *Hawaiite, 3 analyses in Table 1.*

VISUAL DESCRIPTION

Mineralogy: Phenocrysts: essentially aphyric
Groundmass: fine-grained - plag. 50%, px.+op. 35-40%, ol. 10-15%

Lithology: Flow top was up to 30% 5-7 mm vesicles, which become smaller and less abundant downward. Vesicles mostly lined by clay, some calcite filled

Alteration: Mostly moderately fresh. Some olivine is unaltered. Flow bottom is more altered.

THIN SECTION DESCRIPTION

Phenocrysts: Plag. up to 1%, 0.4-0.9 mm, tabular to anhedral

Groundmass: Ol., <1%, 0.05 mm, anhedral, some fresh; plag., 50-60%, 0.1-0.4 mm, variolitic to tabular; cpx. 5-15%, to 0.2 mm, anhedral, skeletal; titanomagnetite, 10%, 0.1-0.4 mm, skeletal to euhedral; apatite, 2%, 0.05 to 0.2 mm, acicular

Texture: Sub-trachytic, sub-ophitic

Vesicles: <1% to 0.5 mm, mostly empty

Alteration: 25% clay after interstitial glass and olivine

MAGNETIC DATA

Average Inclination: −22.3° (±2.8)

Average Magnetic Intensity (10^{-5} Gauss): 474

FLOW UNIT NO. 4:

POSITION: Top - Core 6, Sect. 3, 101 cm; Bottom - Core 6, Sect. 4, 140 cm

CHEMISTRY: Hawaiite, 1 analysis in Table 1.

VISUAL DESCRIPTION

Mineralogy: Phenocrysts: essentially aphyric

Groundmass: 3% altered ol., plag. is 70%, px.+op. 25%, fine-grained

Lithology: Flow top oxidized (5YR 3/3); up to 3 mm vesicles pervasive, but not abundant

Alteration: Moderately fresh

THIN SECTION DESCRIPTION

Phenocrysts: Plag. <1%, 0.7 mm, euhedral; ti-magnetite, <1%

Groundmass: Ol. 3%, 0.05 mm, some fresh cores; plag. 60%, 0.1 mm, laths; cpx. 10%, 0.05 mm, opaques 5%, 0.05 mm; apatite 10%, acicular

Texture: Pilotaxitic to sub-trachytic

Vesicles: None

Alteration: 20% clay after interstitial glass and olivine

MAGNETIC DATA

Average Inclination: −18.9°

Average Magnetic Intensity (10^{-5} Gauss): 631

COMMENTS

Material in Core 6, Sect. 4 was recovered from the bit when the pipe was pulled it fell from the core-catcher when Core 6 was pulled. The pieces are not in their true stratigraphic position.

FLOW UNIT NO. 5

POSITION: Core 6, Sect. 4, pieces 14 and 18

CHEMISTRY: Tholeiitic basalt, 1 analysis in Table 1.

VISUAL DESCRIPTION

Mineralogy: Phenocrysts: 15-20% glomerocrysts of plag. and px., 3 mm across
Groundmass: 70% plag., 25% px., 5% altered ol., fine-grained

Lithology: A few 1-2 mm vesicles filled by green clay

Alteration: Moderately fresh

MAGNETIC DATA

Average Magnetic Intensity (10^{-5} Gauss): 287

Note: No recovery for Cores 7, 8, and 9.

VISUAL CORE DESCRIPTION FOR IGNEOUS ROCKS

LEG 55 SITE 430 HOLE A CORE 10 DEPTH 114.0-117.0 m

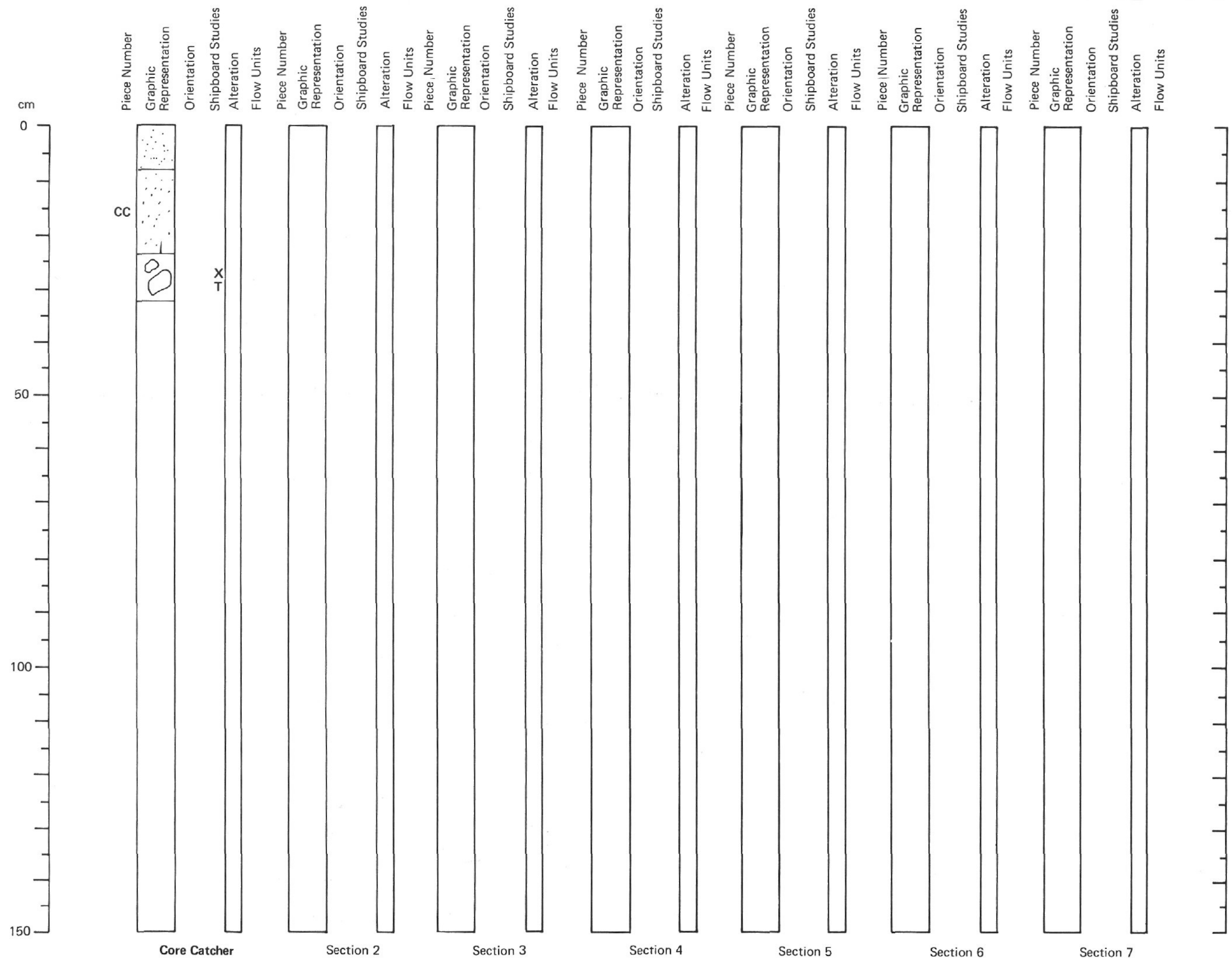

CORE 10 DEPTH 114.0-117.0 m

0-24 cm: Drilling breccia
24-32 cm: Dense hawaiite, probably from Flow Unit 4 or 5

CORE 11 DEPTH 117.0-118.0 m

Aphyric basalt - probably hawaiite from Flow Unit 4 or 5

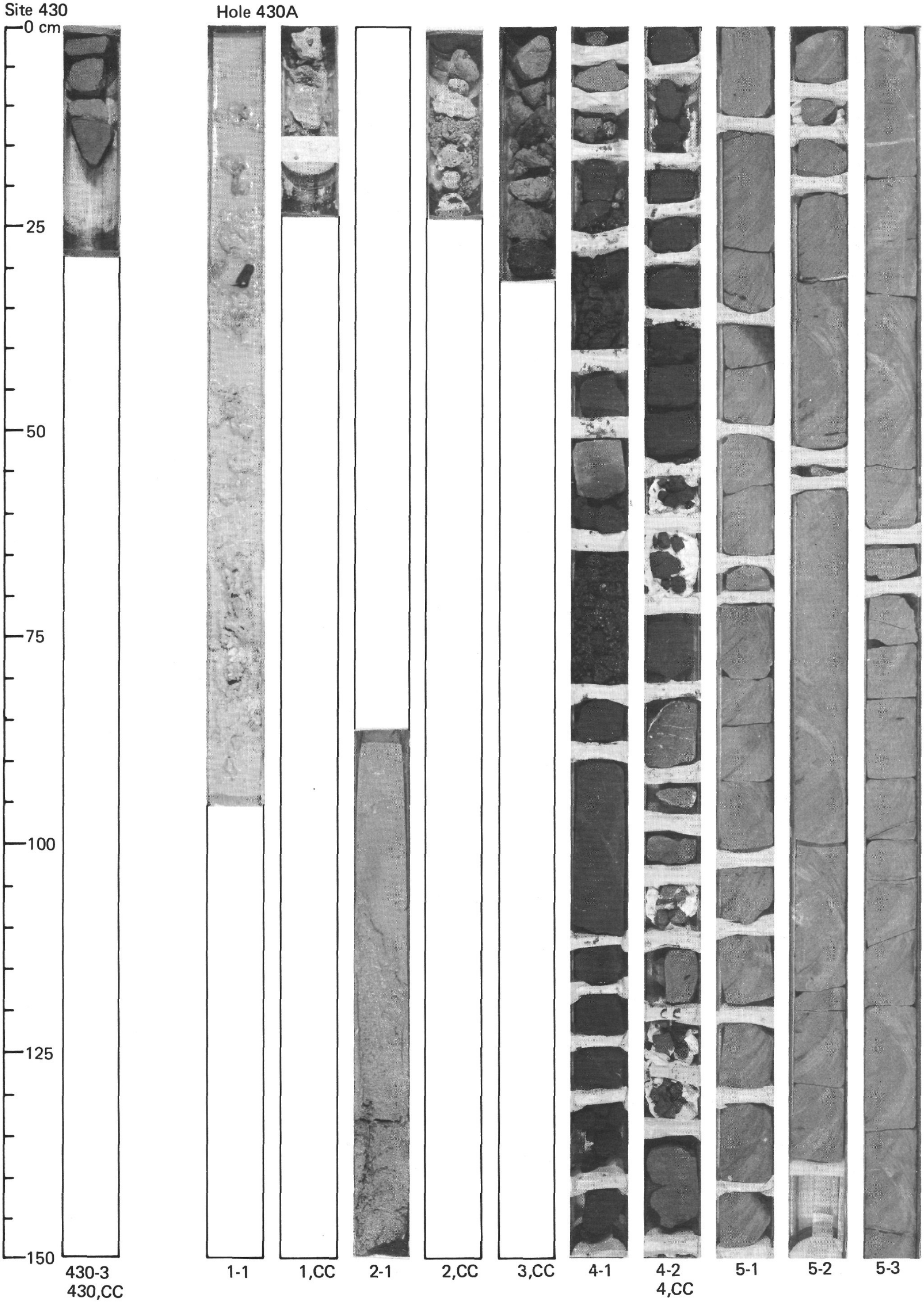
Site 430
Hole 430A
0 cm
25
50
75
100
125
150
430-3
430,CC
1-1
1,CC
2-1
2,CC
3,CC
4-1
4-2
4,CC
5-1
5-2
5-3

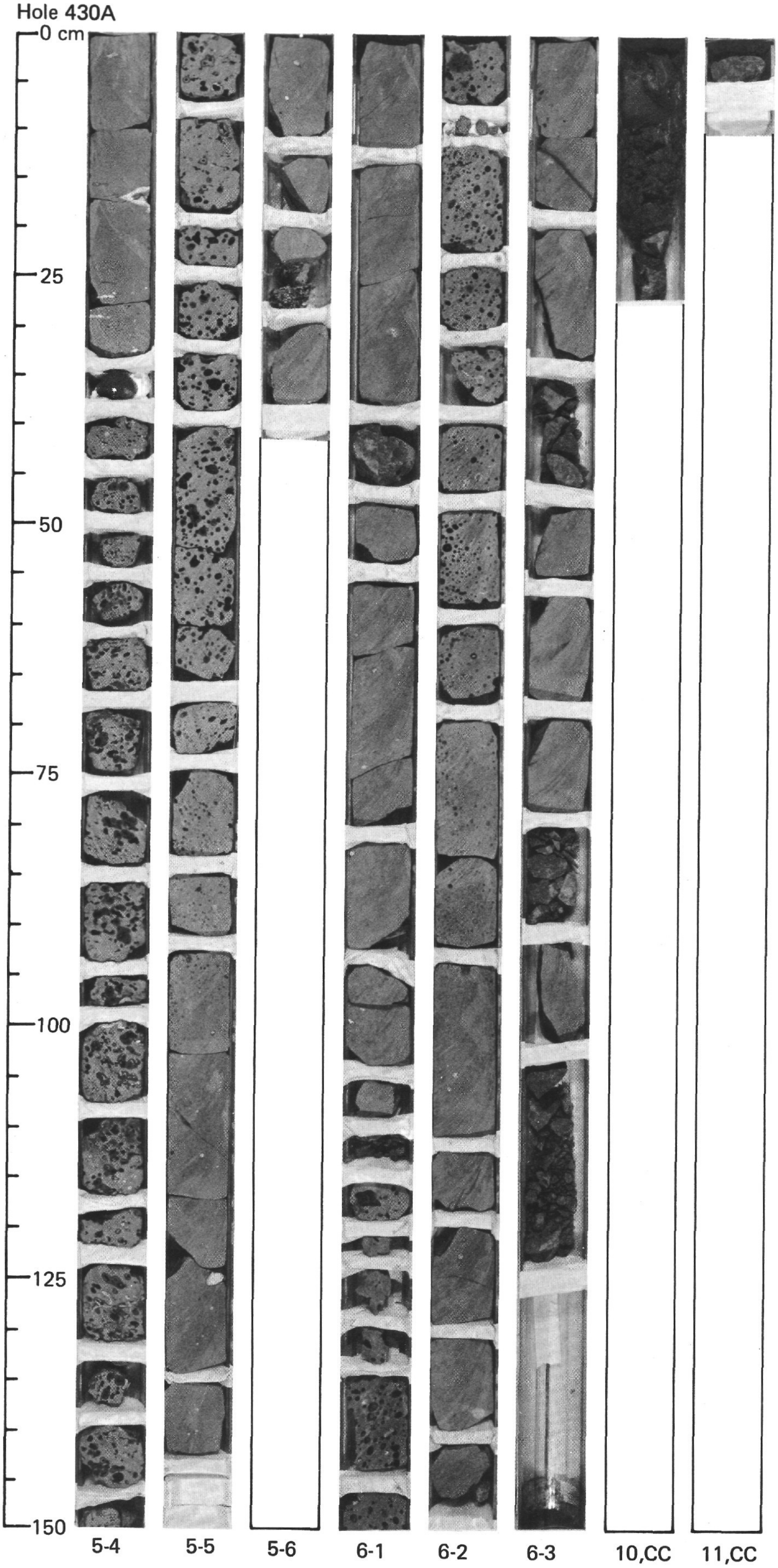
Hole 430A
0 cm
25
50
75
100
125
150
5-4
5-5
5-6
6-1
6-2
6-3
10,CC
11,CC